Title: Arabidopsis uORF-containing mRNAs behave differently from NMD targets

Author Affiliations: Hsin-Yen Larry Wu[1] and Polly Yingshan Hsu[1, #]

[1] Department of Biochemistry & Molecular Biology, Michigan State University, East Lansing, MI 48824 USA

[#] Corresponding author: pollyhsu@msu.edu, phone: 517-353-5284

ORCIDs:

0000-0001-9407-338X (H.L.W.)

0000-0001-7071-5798 (P.Y.H.)

Keywords: translation, upstream open reading frames, nonsense-mediated decay, mRNA half-life, ribosome profiling, Arabidopsis

The author(s) responsible for distribution of materials integral to the findings presented in this article in accordance with the policy described in the Instructions for Authors (https://academic.oup.com/plcell/pages/General-Instructions) is: Polly Hsu (pollyhsu@msu.edu).

Figures 1-5

Supplementary Figures 1-10

Supplementary Tables 1-4

ABSTRACT

Upstream ORFs (uORFs) are common regulatory elements in the 5' untranslated regions of eukaryotic mRNAs. In addition to repressing main ORF translation, uORF translation in animals also reduces mRNA stability through nonsense-mediated decay (NMD). In contrast, the roles of uORFs in plants are less understood. Here, we identified actively translated uORFs (TuORFs) in Arabidopsis through ribosome profiling and systematically examined their roles in gene expression. Like animal systems, Arabidopsis TuORFs are associated with 38%, 14%, and 43% reductions in translation efficiency, mRNA half-lives, and protein levels, respectively. However, we found TuORF-containing mRNAs have 51% higher transcript levels, and this phenomenon is persistent in diverse tissues and developmental stages across plants. We present multiple lines of evidence that indicate Arabidopsis uORF-containing mRNAs generally exhibit distinct behavior from known NMD targets. First, TuORF-containing mRNAs are not increased in NMD mutants. Second, TuORF-containing mRNAs and known NMD targets have distinct expression patterns, and they are translationally repressed via different mechanisms. Finally, TuORF-containing mRNAs and NMD targets are degraded through separate pathways. Our results suggest that Arabidopsis TuORFs reduce mRNA stability and translation through mechanisms different from NMD and highlight a fundamental difference in gene regulation mediated by TuORFs in plants and animals.

INTRODUCTION

Upstream open reading frames (uORFs) are cis-acting translational repressors that regulate many eukaryotic protein-coding transcripts. Mutations or modifications of uORFs are associated with human diseases and plant traits (Calvo et al., 2009; Xu et al., 2017; Zhang et al., 2018; Lee et al., 2021). Considering AUG as a translation start codon, 30%–70% of genes contain at least one potential uORF in moss, Arabidopsis, fly, mouse, and human (Kim et al., 2007; Johnstone et al., 2016; Zhang et al., 2021). Genes with predicted uORFs are enriched for signal transduction proteins, transcription factors, and membrane proteins in animals (Zhang et al., 2021) and for transcription factors and protein kinases in plants (Kim et al., 2007), underlining the potential importance of uORFs in modulating the expression of vital cellular regulators.

Many studies in eukaryotes have reported that uORF translation reduces main ORF (mORF) translation (Chew et al., 2016; Johnstone et al., 2016; Liu et al., 2013; Wu et al., 2019; Lin et al., 2019), and it is estimated to reduce protein production by 30%–80% (Calvo et al., 2009; Chew et al., 2016). According to the scanning model of mRNA translation, the 43S pre-initiation complex, which contains the small ribosomal subunit, several translation initiation factors, and initiator tRNA, binds the 5’ cap and scans the 5’ untranslated region (UTR) to search for an optimal initiation sequence (Hinnebusch et al., 2016). When a uORF is translated, the ribosome may stall during elongation or at termination, or it may dissociate from the mRNA after termination, thus reducing the translation of the downstream mORF (Dever et al., 2020). The mORFs downstream of uORFs may get translated through leaky scanning or reinitiation (Kozak, 1999).

uORF translation is also expected to trigger mRNA degradation, presumably through nonsense-mediated decay (NMD). NMD is an evolutionarily conserved regulatory mechanism to eliminate aberrant mRNAs, such as those that contain premature termination codons or unusually long 3’ UTRs (He and Jacobson, 2015; Kurosaki et al., 2019). Two pathways have been established in mammals: the exon junction complex (EJC)-dependent and long 3’ UTR pathways. Normally, EJC and two NMD factors (UP-FRAMESHIFT SUPPRESSOR 2 and 3; UPF2 and UPF3) deposited during splicing of mRNAs will be evicted by the ribosome in the first round of translation. In the presence of a premature termination codon, EJC-UPF2-UPF3 complexes downstream of the termination codon remain attached to the mRNA. This allows UPF1, which is part of the surveillance complex recruited at translation termination, to interact with UPF2 and UPF3 in proximity. The interaction of UPF1, UPF2, and UPF3 activates the SUPPRESSOR WITH MORPHOLOGICAL EFFECT ON GENITALIA1 (SMG1) kinase, which

79 phosphorylates UPF1. This establishes the first phase of NMD, substrate recognition, and
80 activates downstream signaling and eventually the second phase of NMD, substrate
81 degradation, which involves SMG5, SMG6, and SMG7. Phosphorylated UPF1 also inhibits
82 translation initiation (Isken et al., 2008). Alternatively, unusually long 3' UTRs, which result in
83 poor translation termination, are believed to promote NMD through phosphorylated UPF1
84 independent of EJC (Kurosaki et al., 2014).
85 The plant NMD pathway is best characterized in *Arabidopsis thaliana*. Arabidopsis
86 possesses homologous NMD factors involved in the first phase, including UPF1, UPF2, and
87 UPF3, and in the second phase, SMG7 (Raxwal and Riha, 2016). However, Arabidopsis is
88 missing the homologs of animal SMG1, SMG5, and SMG6 (Lloyd and Davies, 2013). The
89 absence of key NMD components in plants suggests significant variations in the NMD
90 mechanisms between plants and animals. It remains an open question how the differences in
91 NMD components affect substrate recognition and degradation in plants.
92 In Arabidopsis, putative NMD targets have been identified based on transcripts that
93 overly accumulate in NMD-defective mutants (Kurihara et al., 2009; Kalyna et al., 2012;
94 Drechsel et al., 2013; Degtiar et al., 2015). However, there is a concern that the upregulation of
95 some transcripts in NMD mutants might be caused by secondary effects of NMD (Raxwal et al.,
96 2020). For example, NMD mutants affect numerous aspects of plant physiology, and some
97 alleles cause severe growth retardation and lethality due to constitutive immune responses
98 (Jeong et al., 2011; Rayson et al., 2012; Riehs-Kearnan et al., 2012; Filichkin et al., 2015;
99 Merchante et al., 2015; Chiam et al., 2019; Yoine et al., 2006). Moreover, UPF1 has been
100 reported to have multiple functions in plants, such as alternative splicing regulation and
101 translational control, in addition to NMD (Raxwal et al., 2020). To identify *bona fide* NMD
102 targets, *upf1* and *smg7*, which are defective in the first and second phases of NMD,
103 respectively, were introduced into *pad4*, in which the immune response is inactivated (Riehs-
104 Kearnan et al., 2012; Raxwal et al., 2020). The 333 transcripts upregulated in both *upf1 pad4*
105 and *smg7 pad4* were defined as high-confidence NMD targets. It was shown these NMD targets
106 are translationally regulated by UPF1 and that their turnover requires decapping and 5' to 3'
107 decay (Raxwal et al., 2020).
108 As uORF translation could mimic a transcript with an unusually long 3' UTR, uORF-
109 containing mRNAs are predicted to be targeted by NMD (Kertész et al., 2006; Kurosaki et al.,
110 2019). Consistent with this expectation, genome-wide studies in zebrafish, mouse, and human
111 have found that transcripts with translated uORFs have lower mRNA levels globally (Chew et
112 al., 2016; Johnstone et al., 2016). Moreover, transcripts containing translated uORFs are

113 upregulated in knockdown of NMD factors in mouse embryonic stem cells and human cell lines
114 (Hurt et al., 2013; Baird et al., 2018), supporting the idea that these transcripts are NMD targets.
115 In plants, whether uORF translation triggers NMD is still under debate. Two genome-
116 wide studies suggest that uORF-containing mRNAs are targets of NMD, as transcripts
117 possessing predicted uORFs are enriched in the genes upregulated in Arabidopsis *upf1-1* and
118 *upf3-1* mutants (Kurihara et al., 2009; Drechsel et al., 2013). In contrast, three studies
119 suggested that NMD only controls a small fraction of uORF-containing mRNAs in plants, such
120 as those containing uORFs with > 35 codons (~2% of uORF-containing genes), or those
121 responsive to certain environmental stimuli, such as polyamine or blue light (Nyikó et al., 2009;
122 Uchiyama-Kadokura et al., 2014; Kurihara et al., 2018). Moreover, evidence from several gene-
123 specific or genome-wide studies suggests that uORFs do not trigger NMD. First, the mRNA
124 levels of several uORF-containing transcripts, including *NIP5;1* and *AtMHX*, are not increased in
125 NMD mutants (Saul et al., 2009; Tanaka et al., 2016). Second, a genome-wide study reported
126 that genes with increasing numbers of uORFs did not show lower transcript abundances in
127 Arabidopsis and tomato (Li and Liu, 2020). Third, genes with predicted uORFs are not over-
128 represented in the consensus NMD target list identified from three NMD mutants, including
129 *upf1-5*, *upf3-1*, and *smg7-1* (Rayson et al., 2012). It was also reported that 47 mRNAs that
130 contain Conserved Peptide uORFs (CPuORFs) behave differently from NMD targets prior to
131 their degradation mediated by XRN4 (Nagarajan et al., 2019). It is unknown whether some
132 uORF-containing mRNAs escape NMD or whether uORF-containing mRNAs are generally not
133 targets of NMD in plants. It has been concluded that the mRNA features studied so far are
134 insufficient to infer NMD targetability in plants (Ohtani and Wachter, 2019). Overall, it remains
135 unclear how translated uORFs affect mRNA stability and what the role of NMD in this process is
136 in plants.
137 One limitation of the previous studies is that predicted uORFs, which include both
138 translated and untranslated uORFs, were commonly included in the analyses. Although many
139 uORFs have been predicted based on nucleotide sequences (Zhang et al., 2021), determining
140 which uORFs are actively translated still requires experimental evidence. Recently, deep
141 sequencing of ribosome footprints – known as ribosome profiling or Ribo-seq – has been
142 exploited to study genome-wide mRNA translation (Ingolia et al., 2009; Brar and Weissman,
143 2015). Several Ribo-seq studies in Arabidopsis have deployed different strategies to identify
144 translated uORFs (TuORFs) (Liu et al., 2013; Juntawong et al., 2014; Hsu et al., 2016; Hu et al.,
145 2016; Bazin et al., 2017; Kurihara et al., 2020). Among the parameters used, 3-nucleotide (3-nt)
146 periodicity, which corresponds to translating ribosomes deciphering 3 nts per codon, is

147 considered the most stringent criterion to identify high-confidence translation events (Ingolia et
148 al., 2009; Calviello et al., 2016; Xu et al., 2018; Harnett et al., 2021). Our previous work and a
149 recent study using RiboTaper (Calviello et al., 2016), which computes the statistical significance
150 of 3-nt periodicity, uncovered 187–1378 AUG-initiated TuORFs in Arabidopsis (Hsu et al., 2016;
151 Kurihara et al., 2020).

152 Here we further improved the Ribo-seq methodology and identified 2093 AUG-initiated
153 TuORFs in Arabidopsis seedlings. We systematically examined the assumed roles of TuORFs
154 in mORF translation and mRNA decay by integrating multiple genome-wide datasets. As
155 predicted, we found that TuORF mRNAs are associated with lower translation efficiency, shorter
156 mRNA half-lives, and lower protein abundance. Surprisingly, we found that, in contrast to the
157 animal paradigm, plant TuORF mRNAs are associated with higher steady-state mRNA levels,
158 and they are not increased in the NMD mutants. Examinations of additional parameters
159 revealed that uORFs and NMD regulate gene expression through separate mechanisms. Taken
160 together, our results reveal unexpected features and regulation of uORFs in Arabidopsis and
161 suggest that plants and animals have evolved different uORF-dependent mechanisms for gene
162 regulation.

RESULTS

Translated uORFs identified via an improved Ribo-seq method

Previously we optimized Ribo-seq to reach high 3-nt periodicity, and we exploited this unique feature of mRNA translation to identify translated ORFs in Arabidopsis (Hsu et al., 2016). Although the data revealed many unannotated translation events, the number of TuORFs uncovered was low, presumably due to insufficient Ribo-seq coverage within uORFs. We proposed that increasing Ribo-seq coverage could improve the efficiency of translated ORF identification, especially for relatively short ORFs, such as uORFs. Here we optimized the coverage of Ribo-seq in 7-day-old Arabidopsis seedlings by minimizing the potential loss of ribosome footprints during the purification process (see METHODS for details).

In addition to high correlations among biological replicates (**Figure S1A**), our new Ribo-seq data displayed characteristics expected for high-quality data, including strong 3-nt periodicity (92% in-frame reads), high enrichment for coding sequences (CDSs), and characteristic ribosome footprint lengths (**Figure 1A-C**). The improved coverage is evident when examining the number of unique ribosome footprints detected globally. At a sequencing depth of 20 million reads from randomly selected reads, the number of unique ribosome footprints in our new data is 4.01-fold higher than that in our previous dataset (**Figure 1D**). The coverage improvement is also evident in individual transcript profiles within both uORF and mORF regions. For example, a TuORF in *REPRESSOR OF GA1* (*RGA1*) was identified in our current data but missed in our previous study despite the mRNA levels being similar (**Figure S1B**).

The high-coverage data increased the number of TuORFs uncovered. In total, 2093 TuORFs were identified in 1768 genes based on significant 3-nt periodicity using RiboTaper (with the default cutoff of RiboTaper, Multitaper F-test, $p < 0.05$) and Araport11 annotation (**Figure 1E** and **Table S1A**). This result is in strong contrast to the relatively few TuORFs identified in Arabidopsis seedling shoots (93 TuORFs) and roots (138 TuORFs) from our previous data obtained using plants grown under similar conditions and using the same statistical analysis and annotations (**Figure 1E** and **Table S1B-C**). The new data also revealed translation from a higher number of Conserved Peptide uORFs (CPuORFs) and annotated coding sequences (mORFs of protein-coding genes) (**Figure 1E** and **Table S1D-F**). We manually plotted all TuORF genes to confirm strong 3-nt periodicity present in the expected uORF regions using RiboPlotR (Wu and Hsu, 2021) (examples shown in **Figure 1F-G, Figure S2**). Taken together, these results show that our enhanced-coverage Ribo-seq data dramatically improved the identification of TuORFs.

196 Previous analyses of predicted uORFs found that transcription factors and protein
197 kinases are overrepresented among uORF-containing genes (Von Arnim et al., 2014; Kim et al.,
198 2007). Consistent with these analyses, functions related to transcription factors and protein
199 kinases/phosphatases were identified as being enriched in our Gene Ontology (GO) analysis of
200 TuORF-containing genes (**Table S2**). We found that many TuORF-containing genes encode
201 extensively studied regulators of plant growth and environmental responses. For example, this
202 list included well-known transcription factors, such as those involved in hormone signaling
203 (RGA1 and AUXIN RESPONSE FACTOR2/3/8), root development (SCARECROW), the
204 circadian clock (TIMING OF CAB EXPRESSION1), and light signaling (PHYTOCHROME
205 INTERACTING FACTOR3/4/7) (Silverstone et al., 1998; Strayer et al., 2000; Di Laurenzio et al.,
206 1996; Ellis et al., 2005; Nagpal et al., 2005; Ni et al., 1998; Huq and Quail, 2002; Leivar et al.,
207 2008). The list also included well-characterized protein kinases, such as Phytochromes B and
208 E, ribosomal-protein S6 kinases (S6K1/2), and SNF1-related protein kinase 2 (SNRK2.1/2.5)
209 (**Figure S1B, S2A-N**) (Sharrock and Quail, 1989; Devlin et al., 1998; Zhang et al., 1994;
210 Mizoguchi et al., 1995; Park et al., 1993; Boudsocq et al., 2004). These results support the
211 notion that TuORFs control important cellular regulators in plants.
212
213 **TuORF-containing genes have higher mRNA abundance but are associated with lower**
214 **translation efficiency, shorter mRNA half-lives, and lower protein abundance**
215 To understand how uORF translation affects gene expression, we compared mRNA
216 abundance and translation efficiency of TuORF-containing genes (hereafter, TuORF genes),
217 genes containing sequence-predicted uORFs but undetected by RiboTaper (hereafter, UuORF
218 genes), and genes containing an annotated 5' UTR but no potential uORFs (hereafter, no-uORF
219 genes). Note that some UuORFs may be translated but missed in our analysis because their 3-
220 nt periodicity is insufficient to pass the statistical test: these include extremely short uORFs,
221 those translated at a low frequency, and those overlapping with mORF or other uORFs and thus
222 disrupting the 3-nt periodicity. To study the global effects of uORFs on mRNA stability and
223 protein abundance, we also compared genes with TuORFs, UuORFs, or no-uORFs, using
224 available mRNA half-life data determined by metabolic labeling in Arabidopsis seedlings and
225 two quantitative proteomics datasets from shoots and roots of Arabidopsis seedlings (Szabo et
226 al., 2020; Song et al., 2018). The growth conditions and source of the data are summarized in
227 **Table S3**. Below we presented the data in cumulative plots to show the trends of different gene
228 groups and in box plots to show the statistical results (**Figure 2A-H and S3**).

229 Studies in vertebrates have shown that uORF translation is associated with lower
230 steady-state mRNA abundance, consistent with the expectation that TuORF mRNAs are
231 regulated by NMD (Chew et al., 2016; Johnstone et al., 2016). Surprisingly, we found that
232 TuORF genes in Arabidopsis are associated with higher steady-state mRNA levels than those
233 of UuORF and no-uORF genes (**Figure 2A, 2E**), despite having shorter mRNA half-lives as
234 expected (**Figure 2C, 2G**). The median mRNA level of TuORF genes is 51% higher than that of
235 no-uORF genes (**Figure 2E**). The higher steady-state mRNA levels and shorter mRNA half-lives
236 together suggest that TuORF genes are highly transcribed. To examine whether the high
237 transcript levels of TuORF genes are conserved in other plant species, we reanalyzed our
238 previous tomato Ribo-seq data from seedling roots (Wu et al., 2019) and found the TuORF
239 genes in tomato also have higher steady-state mRNA levels relative to no-uORF genes (**Figure**
240 **S4A**). Given that Arabidopsis and tomato diverged more than 100 million years ago (Clarke et
241 al., 2011), our results suggest that TuORF-associated higher mRNA abundance could be
242 prevalent in plants. To investigate whether our observation is specific to seedlings or common to
243 different developmental stages/tissues/genetic backgrounds in Arabidopsis and tomato, we
244 examined the mRNA levels of the uORF-containing genes in 128 independent RNA-seq studies
245 collected by the EMBO-EBI expression atlas (Papatheodorou et al., 2020). Consistent with our
246 Arabidopsis seedlings and tomato seedling root data, we found the TuORF genes are
247 associated with higher mRNA levels in diverse tissues, developmental stages, and ecotypes in
248 Arabidopsis and tomato (**Figure 2I and S5A-C**), supporting the hypothesis that TuORF genes
249 are preferentially expressed at high levels in these plants under a wide range of sampling
250 conditions.
251 CPuORFs are uORFs that encode evolutionarily conserved peptides, and they were
252 identified independently from our approach by evolutionary conservation (Hayden and
253 Jorgensen, 2007; Jorgensen and Dorantes-Acosta, 2012; Takahashi et al., 2012; Vaughn et al.,
254 2012; Van Der Horst et al., 2019). Many CPuORFs were also identified as TuORFs in our study
255 (**Figure 1E, 1G**). We found that the median mRNA abundance of CPuORF genes is 2.2-fold of
256 that of no-uORF genes (**Figure S6**), consistent with our observations that genes with TuORFs
257 are expressed at higher levels.
258 Next, we examined the translation efficiency, mRNA half-lives, and protein levels of
259 TuORF, UuORF, and no-uORF genes. Consistent with the animal studies, we found
260 Arabidopsis TuORF genes are associated with lower translation efficiency, shorter mRNA half-
261 lives, and less protein accumulation than UuORF and no-uORF genes (**Figure 2B-D, 2F-H, S3,**
262 **S4B**). Interestingly, even though globally TuORF genes start with 51% more mRNAs than no-

263 uORF genes (**Figure 2E**), they produce 41%–43% less protein (**Figure 2H, S3**), on average,
264 likely due to the combined effects of a 38% reduction in translation efficiency (**Figure 2F**) and a
265 14% reduction in mRNA half-lives (**Figure 2G**). These observations suggest that the global
266 repression of TuORF gene protein synthesis is determined by multilayer post-transcriptional
267 regulation. Notably, for the four parameters examined here, UuORF genes consistently have
268 levels between those of TuORF genes and no-uORF genes: they show a 4% increase in mRNA
269 levels and 11%, 6%, and 21% reductions in translation efficiency, mRNA half-lives, and protein
270 abundance, respectively (**Figure 2A-H**). These results indicate that UuORFs have smaller
271 effects on gene expression than TuORFs and highlight the importance of distinguishing
272 TuORFs and UuORFs in genome-wide analysis.
273
274 **TuORF genes are larger and likely evolutionarily older than other genes**
275 We next investigated whether there are general structural differences among TuORF,
276 UuORF, and no-uORF mRNAs. Considering the directionality of ribosome scanning, we
277 hypothesized TuORFs might be associated with longer 5' UTRs. Indeed, we found that the
278 median 5' UTR length of TuORF mRNAs is 2.5-fold of that of no-uORF mRNAs (**Figure S7A**),
279 which is consistent with a previous report that uORFs in longer 5' UTRs are more likely to be
280 translated (Liu et al., 2013). However, unexpectedly, we found that TuORF mRNAs also have
281 longer CDSs and 3'UTRs, as well as longer transcript lengths, than UuORF mRNAs (**Figure**
282 **S7B-D**). No-uORF mRNAs are the shortest in all categories examined (**Figure S7A-D**). These
283 results support the hypothesis that TuORFs are more likely to be found in longer 5' UTRs and
284 reveal that TuORF mRNAs tend to encode larger proteins (**Figure S7B**). The enrichment of
285 TuORF genes for transcription factors, protein kinases, and related functions in GO term
286 analysis (**Table S2**) also implies TuORF genes tend to encode proteins with conserved
287 domains. It is known that evolutionarily older genes are generally longer, expressed at higher
288 levels, and have protein sequences that are under stronger purifying selection (Wolfa et al.,
289 2009; Cui et al., 2015). Our observations that TuORF genes possess many features of
290 evolutionarily older genes imply that older genes are more likely to be regulated through mRNA
291 translation and degradation mediated by TuORFs.
292
293 **TuORF mRNAs are not upregulated in the NMD mutants**
294 The established paradigm in vertebrates is that uORF translation triggers NMD and thus
295 results in low steady-state mRNA levels (Chew et al., 2016; Johnstone et al., 2016; Hurt et al.,
296 2013; Baird et al., 2018). Despite having higher steady-state mRNA levels (**Figure 2A and 2E**),

297 TuORF genes in Arabidopsis also have shorter mRNA half-lives (**Figure 2C and 2G**).
298 Therefore, we investigated whether TuORF-containing transcripts in Arabidopsis are still subject
299 to NMD.
300 If TuORFs trigger NMD, one would expect TuORF mRNAs to be among the known NMD
301 targets and their mRNA levels to be increased in NMD-deficient mutants. We first examined
302 whether TuORF mRNAs were reported in the high-confidence NMD target list (Raxwal et al.,
303 2020). Among the 333 NMD targets that were upregulated in both *upf1 pad4* and *smg7 pad4*
304 adult leaves (Raxwal et al., 2020), 248 genes with an annotated 5' UTR were expressed in our
305 data (**Table S4A**). However, only 49 of 1748 TuORF genes were identified in the high-
306 confidence NMD target list (**Table S4B**). The 49 genes represent 2.8% of TuORF-containing
307 genes and 20% of the NMD targets. These results suggest that TuORFs generally do not trigger
308 NMD; rather, NMD targets are more likely to be regulated by TuORFs than other genes (Chi-
309 square test with Yates' correction: p-value = 7.555e-10). One caveat is that the poor overlap
310 between the two gene lists could be due to differences in growth conditions, developmental
311 stages, and sample handling in different labs (**Table S3**).
312 To further investigate if TuORF mRNAs are NMD targets, we examined whether they are
313 upregulated in NMD-deficient mutants by analyzing four published RNA-seq datasets for NMD
314 mutants (Drechsel et al., 2013; Merchante et al., 2015; Raxwal et al., 2020; Gloggnitzer et al.,
315 2014). Although these datasets were collected from different NMD mutants and at various
316 developmental stages (**Table S3**), the high-confidence NMD targets are consistently and
317 significantly upregulated in all the NMD mutants examined compared with the control plants
318 (i.e., 3.05-, 1.54-, 4.98-, and 2.65-fold for NMD targets without TuORFs; 3.04-, 2.23-, 5.04-, and
319 2.66-fold for NMD targets with TuORFs) (**Figure 3A-D**). In contrast, TuORF mRNA levels show
320 no or little change in the NMD mutants (i.e., 1.01-, 0.98-, 1.10- and 1.10-fold). Thus, only the
321 NMD targets, but not TuORF mRNAs, are dramatically increased in the NMD mutants,
322 supporting the idea that uORF translation in Arabidopsis may not trigger NMD.
323 Given different uORFs are translated at various levels (See **Figure 1F-G, S1B, S2A-N**
324 for examples), it is possible only the highly repressive TuORFs efficiently trigger NMD. To test
325 this hypothesis, we split the TuORF genes into two groups based on their uORF relative
326 translation efficiency (RTE) (i.e., TE of an uORF is normalized to TE of its mORF). However,
327 even the higher TuORF RTE group shows no or little effects on the mRNA accumulation in the
328 NMD mutants (i.e., 1.13-, 0.99-, 1.15- and 1.11-fold) (**Figure 3E-H**). We also tested whether
329 having more TuORFs in a transcript efficiently triggers NMD by splitting the TuORF genes into
330 two groups based on the number of TuORFs detected. We found that even transcripts with 2~5

331 TuORFs do not lead to significant mRNA increase in the NMD mutants, either (i.e., 0.93-, 0.98-,
332 0.99- and 1.09-fold)(**Figure 3I-L**). Together, these results support the idea that NMD is not a
333 major mechanism for controlling uORF-containing mRNAs.
334
335 **Lengths of the TuORF and 3' UTR alone are insufficient to predict NMD targetability**
336 A previous study suggested that uORFs that encode a peptide longer than 35 amino
337 acids are likely to trigger NMD in Arabidopsis (Nyikó et al., 2009). To test whether TuORF
338 length is associated with NMD targetability, we analyzed TuORF lengths in the NMD targets and
339 non-NMD targets. We found that the NMD target TuORF genes tend to have longer uORF
340 peptides than non-NMD target TuORF genes (median length 28 amino acids vs. 20.5 amino
341 acids, p = 9.874e-07, Wilcoxon signed-rank test). However, the distributions of the uORF
342 peptide lengths in NMD targets and non-NMD targets largely overlap (**Figure S8**), indicating
343 that TuORF length alone is insufficient to predict whether a TuORF triggers NMD of a transcript.
344 We also examined whether the high-confidence NMD targets have longer 3' UTRs, a
345 feature that potentially triggers NMD. We found that the NMD targets do not have significantly
346 longer 3' UTRs, regardless of whether they contain TuORFs (**Figure S9**). Taken together, our
347 results are consistent with the notion that no definite RNA features studied to date are sufficient
348 to predict NMD targets in plants (Ohtani and Wachter, 2019).
349
350 **TuORF mRNAs and NMD targets have distinct expression patterns**
351 To further characterize the roles of NMD and TuORFs in gene expression regulation, we
352 compared the expression patterns of the NMD targets and TuORF mRNAs (**Figure 4**).
353 Consistent with the expectation that NMD targets are being actively degraded, we found that
354 NMD targets have lower mRNA abundance than other mRNAs; this is in strong contrast to
355 TuORF mRNAs, which have higher mRNA abundance than other mRNAs (**Figure 4A, 4E**).
356 While both NMD targets and TuORF mRNAs are associated with lower translation efficiency,
357 shorter mRNA half-lives, and lower protein abundance than other mRNAs (**Figure 4B-D, 4F-H**),
358 the NMD targets are associated with even lower protein levels than TuORF mRNAs (**Figure 4D,**
359 **4H**).
360 If TuORFs effectively trigger NMD, one would expect TuORF mRNAs to have translation
361 efficiency similar to that of NMD targets with TuORFs, which would inherently be repressed by
362 both TuORFs and NMD. However, we found that NMD targets with TuORFs have significantly
363 lower translation efficiency than either NMD targets without TuORFs or TuORF mRNAs not
364 identified as NMD targets (**Figure 4B, 4F**). This additive repression of translation efficiency in

365 NMD targets with TuORFs suggests that NMD and TuORFs suppress translation through
366 separate mechanisms. This result also supports that TuORFs do not effectively trigger NMD.
367 Our observation is consistent with the expectation that TuORFs prevent the scanning pre-
368 initiation complex from reaching the mORF, while NMD suppresses translation through UPF1
369 and/or other translational repressors (Isken et al., 2008; Raxwal et al., 2020; Zinshteyn et al.,
370 2021).
371 Together, the differences in the expression patterns between TuORF mRNAs and NMD
372 targets further support the idea that TuORF mRNAs behave differently from NMD targets in
373 Arabidopsis.
374
375 **TuORF mRNAs and NMD targets are degraded through different mRNA decay**
376 **mechanisms**
377 We next investigated the mechanisms underlying the decay of TuORF mRNAs and NMD
378 targets. mRNA decay can occur in the 5' to 3' or 3' to 5' direction, which is carried out by
379 different machinery (Sieburth and Vincent, 2018). A genome-wide survey of mRNA decay rates
380 in wild type and mutants defective in either 5' to 3' decay or 3' to 5' decay, or both, has been
381 conducted in Arabidopsis (Sorenson et al., 2018). In that survey, the *vcs-7* mutant, a null mutant
382 of *VARICOSE*, which encodes a scaffold protein for the mRNA decapping complex, was used to
383 examine the 5' to 3' mRNA decay; the *sov* mutant, defective in *SUPPRESSOR OF VARICOSE*,
384 which encodes a ribonuclease II, was used to examine 3' to 5' decay; and the *vcs/sov* double
385 mutant was used to examine decay affected in both directions (Deyholos et al., 2003; Goeres et
386 al., 2007; Xu et al., 2006; Zhang et al., 2010). We exploited this published dataset (Sorenson et
387 al., 2018) to study the genetic requirements for the mRNA decay of TuORF mRNAs, NMD
388 targets, TuORF-containing NMD targets, and other mRNAs.
389 We first compared the decay rates of each gene group across the four genetic
390 backgrounds (**Figure 5**). Similar to mRNAs that are non-NMD targets and lack TuORFs (i.e.,
391 other mRNAs, **Figure 5D, 5H**), TuORF mRNAs have dramatically reduced decay rates in the
392 *vcs* mutant compared to the wild type (**Figure 5A, 5E**), indicating that decapping and 5' to 3'
393 decay are critical for degrading these transcripts. In the *vcs/sov* double mutant, TuORF mRNAs
394 have slightly but significantly lower decay rates than in the *vcs* mutant (**Figure 5A and 5E**),
395 suggesting *SOV* also plays a minor role in degrading TuORF mRNAs.
396 In contrast, the mRNA decay rates of NMD targets without TuORFs are only significantly
397 lower in the *vcs/sov* double mutant (**Figure 5B, 5F**), suggesting that NMD targets can be
398 efficiently degraded by either the 5' to 3' or 3' to 5' pathways. In other words, in the absence of

399 either *SOV* or *VCS*, the remaining pathway could completely take over the decay of NMD
400 targets (**Figure 5B, 5F**). Although there are fewer NMD targets containing TuORFs, which
401 resulted in small sample size and statistical insignificance (**Figure 5C, 5G**), the decay rates in
402 this group of genes in the four genetic backgrounds show trends similar to other NMD targets
403 without TuORFs (**Figure 5B, 5F**).
404 Next, we compared the decay rates of the four gene groups within each genetic
405 background (**Figure S10)**. In all four genetic backgrounds, NMD targets with or without TuORFs
406 consistently have higher decay rates than TuORF mRNAs and other mRNAs (**Figure S10A-H**).
407 This pattern is still persistent in the *vcs/sov* double mutant **(Figure S10D, S10H)**, suggesting
408 additional decay pathway(s) is involved in degrading the NMD targets in the absence of both
409 VCS and SOV.
410 Taken together, our results suggest that TuORF mRNAs and NMD targets are
411 preferentially degraded through different decay pathways. Furthermore, NMD targets
412 consistently have higher decay rates than TuORF mRNAs and appear to be regulated by
413 additional pathway(s) other than VCS and SOV (see the model in **Figure 5I**).
414
415 **DISCUSSION**
416 In this study, we identified Arabidopsis TuORFs using improved Ribo-seq data and
417 systematically examined their roles in gene expression. While our results support the expected
418 roles of uORFs in repressing mORF translation and mRNA stability, our study reveals distinct
419 features and regulation of uORFs in plants compared with animals.
420 Our observations that plant TuORF genes are associated with higher expression levels
421 (**Figure 2**), encode larger proteins (**Figure S7B**), and are enriched for evolutionarily conserved
422 domains (**Table S2**) raised an interesting question as to whether older genes are more likely to
423 be controlled at the protein levels through mRNA degradation and translation via uORFs. Higher
424 mRNA abundance may allow TuORF mRNAs to be highly translated under certain conditions
425 that require a high level of specific proteins. For example, it has been suggested that
426 derepression of downstream translation is a general mechanism of uORF-mediated expression
427 under stress (Andreev et al., 2018). Thus, TuORFs could enable fast and dynamic regulation of
428 mORF translation. Future work monitoring the translation of TuORFs and their mORFs under
429 different conditions will help decipher the regulation and physiological roles of specific TuORFs.
430 If TuORFs trigger NMD in Arabidopsis, we would expect that TuORF mRNAs behave
431 similarly to NMD targets. In this report, we presented six observations suggesting that
432 Arabidopsis TuORF mRNAs and NMD targets are two distinct groups of transcripts: (1) NMD

433 targets, but not TuORF mRNAs, are upregulated in various NMD mutants (**Figure 3**). (2)
434 TuORF mRNAs have significantly higher transcript levels, while the NMD targets have lower
435 transcript levels than other genes (**Figure 4A and 4E**). (3) NMD and TuORFs additively repress
436 translation, suggesting they repress translation through separate mechanisms (**Figure 4B, 4F**).
437 (4) While NMD targets are efficiently degraded through both 5' to 3' and 3' to 5' decay, TuORF
438 mRNAs, like other genes, mainly rely on 5' to 3' decay (**Figure 5**). (5) The decay rates of NMD
439 targets are consistently higher than those of TuORF mRNAs (**Figure S10)**. (6) NMD targets also
440 appear to be degraded by additional pathway(s) in the absence of both *VCS* and *SOV* (**Figure**
441 **S10H**). These differences between TuORF mRNAs and NMD targets suggest that NMD is not a
442 major mechanism regulating TuORF mRNAs.
443 The fact that Arabidopsis is missing key NMD factors found in animals, including SMG1,
444 SMG5, and SMG6, suggests significant variations in the NMD mechanisms between plants and
445 animals. In particular, SMG1 is the kinase responsible for UPF1 phosphorylation required for
446 substrate recognition in animal NMD (He and Jacobson, 2015; Kurosaki et al., 2019). The lack
447 of SMG1 and the use of an alternative kinase for Arabidopsis UPF1 phosphorylation (Kerényi et
448 al., 2013) may lead to a difference in substrate recognition: while TuORF mRNAs are
449 recognized as NMD targets in animals, plant TuORF mRNAs are not.
450 Despite the difference in NMD components in plants and animals, our findings that
451 Arabidopsis NMD targets are degraded through both 5' to 3' decay and 3' to 5' decay is
452 consistent with the two-directional decay of NMD targets in animals. Note that plant SOV is the
453 homolog of DIS3L2, the exonuclease responsible for 3' to 5' decay of NMD targets in animals
454 (Chang et al., 2013; Lubas et al., 2013). Two-directional decay could be advantageous to
455 quickly remove aberrant mRNAs from the cytoplasm to prevent further translation and facilitate
456 the recycling of NMD machinery.
457 It is well established that there is an important interplay between translation efficiency
458 and mRNA stability. Two mechanisms have been proposed to explain this phenomenon: the
459 "stalled ribosome-triggered decay model," which predicts that ribosome stalling or slowing
460 promotes mRNA degradation, and the "translation factor-protected model," which predicts that
461 active translation promotes mRNA stability because the translation initiation factors protect the
462 mRNA from the decapping complex (Presnyak et al., 2015; Radhakrishnan et al., 2016;
463 Beelman and Parker, 1994; LaGrandeur and Parker, 1999; Schwartz and Parker, 2000; Chan et
464 al., 2018). Consistent with the first model, several CPuORF-containing mRNAs in Arabidopsis
465 were reported to have strong ribosome stalling patterns, and the endonucleolytic cleavages
466 upstream of the stalled ribosomes were observed (Hou et al., 2016; Yu et al., 2016). While most

467 of the TuORFs we identified did not display clear stalling patterns (e.g., **Figure 1F-G, S1B,**
468 **S2A-N**), it remains possible that ribosomes have lower translation speeds, on average, during
469 uORF translation. Because ribosomes will quickly approach termination after initiation due to the
470 short length of uORFs, and because both initiation and termination are major time-consuming
471 steps in translation (Shah et al., 2013; Lawson et al., 2021), the average translation speed per
472 codon for uORFs is likely to be slower than that for longer ORFs. Alternatively, if cells mainly
473 monitor the translation efficiency of the mORF, then the poorer mORF translation caused by
474 uORFs could explain the faster degradation of TuORF mRNAs predicted by this model. In
475 contrast, since ribosomes actively engage with TuORFs, the “translation factor-protected” model
476 does not fit TuORF mRNAs, especially because their degradation relies on decapping and 5’ to
477 3’ decay in plants. Further investigation into TuORF-mediated mRNA degradation will help
478 elucidate the role of uORFs in regulating mRNA stability.
479

480 **METHODS**

481 **Plant growth conditions and lysate preparation**

482 Arabidopsis Col-0 seeds were surface sterilized with 70% ethanol for 5 min, followed by 33%
483 bleach and 0.03% Tween 20 for 10 min, then rinsed with sterile water 5 times. The seeds were
484 imbibed at 4°C in the dark for 2 days, then grown hydroponically in sterile liquid media (2.15 g/L
485 Murashige and Skoog salt, 1% sucrose, 0.5 g/L MES, pH 5.7) while shaking at 85 rpm under a
486 16-h light (75–80 μmol $m^{-2} \cdot s^{-1}$ from cool white fluorescent bulbs) and 8-h dark cycle at 22°C for
487 7 days. At Zeitgeber time 4 (4 h after lights on), DMSO corresponding to 0.1% of the media
488 volume was added to the media (these were mock samples of our large-scale experiment). After
489 20 and 60 min, three biological replicates (~300 plants per sample) were harvested at each time
490 point and immediately flash frozen in liquid nitrogen.

491

492 Plant lysates were prepared as previously described (Hsu et al., 2016). Briefly, per 0.1 g of
493 ground tissue powder was resuspended in 400 μL of lysis buffer (100 mM Tris-HCl [pH 8], 40
494 mM KCl, 20 mM $MgCl_2$, 2% [v/v] polyoxyethylene [10] tridecyl ether [Sigma, P2393], 1% [w/v]
495 sodium deoxycholate [Sigma, D6750], 1 mM dithiothreitol, 100 μg/mL cycloheximide [Sigma,
496 C4859], 100 μg/mL chloramphenicol [Sigma R4408], and 10 units/mL DNase I [Epicenter,
497 D9905K]). The lysates were spun at 3,000 g for 3 min, and the supernatant was transferred to a
498 new tube and subsequently centrifuged at 20,000 g for 10 min. The supernatant was transferred
499 to a new tube and the RNA concentration was determined with 10x dilutions using the Qubit
500 RNA HS assay (Thermo Fisher Scientific; Q32852). Aliquots of 100 μL and 200 μL of the
501 lysates were made, and they were flash frozen in liquid nitrogen and stored at -80°C until further
502 processing.

503

504 **Ribo-seq library construction**

505 Ribosome footprints were obtained using 200 μL of the lysates described above, and
506 sequencing libraries were constructed according to our previous method (Hsu et al., 2016) with
507 the following modifications: briefly, after RNase I digestion (50 units nuclease per 40 μg of RNA;
508 the nuclease was included in TruSeq Mammalian Ribo Profile Kit, Illumina, RPHMR12126),
509 adding 15 μl of SUPERase-IN (Invitrogen, AM2696), and passing through a size exclusion
510 column (Illustra MicroSpin S-400 HR Columns; GE Healthcare; 27-5140-01), RNA > 17 nt was
511 isolated with the RNA Clean & Concentrator-25 kit (Zymo Research, R1017) and separated on
512 15% urea-TBE gels (Invitrogen, EC68852BOX). Gel slices between 28 and 30 nt were isolated,
513 and the RNAs were purified as previously described. Next, rRNA depletion was performed using

514 RiboZero Plant Leaf kit (Illumina, MRZPL1224) in one quarter of the recommended reaction
515 volume. The major change we made here was to gel-purify the ribosome footprints prior to the
516 rRNA depletion. In our previous protocol, we purified the RNA twice (first >17 nt and then <200
517 nt) to enrich ribosome footprints before the rRNA depletion and gel purification. We reasoned
518 that some footprints might be lost during the two RNA purification steps. In addition, the rRNA
519 depletion step requires a limited amount of input RNA according to the manufacturer's
520 recommendations. Therefore, we expected modifying the order of these steps could maximize
521 the input and minimize the footprint loss during the processes. Ribo-seq libraries were then
522 constructed using the TruSeq Mammalian Ribo Profile Kit (illumina, RPHMR12126) as
523 previously described with nine cycles of PCR amplification. Libraries with equal molarity were
524 pooled and sequenced on a Hi-Seq 4000 sequencer using single-end 50-bp sequencing.
525
526 **RNA-seq library construction**
527 Total RNA greater than 200 nt was purified from 100 μL of the lysates described above using
528 the RNA Clean & Concentrator-25 kit (Zymo Research, R1017) as previously described (Hsu et
529 al., 2016). RNA integrity was evaluated using a Bioanalyzer (Agilent) RNA pico chip, and RNA
530 integrity numbers (RINs) ranging from 7.2 to 7.7 were observed among the samples. A total of 4
531 μg of RNA per sample was subjected to rRNA depletion using the RiboZero Plant Leaf kit
532 (Illumina, MRZPL1224) following the manufacturer's recommendations. Then, 100 ng of rRNA-
533 depleted RNA was fragmented to around 200-nt long based on the RIN reported by the
534 Bioanalyzer, and strand-specific sequencing libraries were made using the NEBNext Ultra II
535 Directional RNA Library Prep Kit (New England Biolabs, E7760S) with eight cycles of
536 amplification. Libraries of equal molarity were pooled and sequenced on a Hi-Seq 4000 using
537 paired-end 100-bp sequencing.
538
539 **Data pre-processing and analysis**
540 Data pre-processing and analysis were performed similarly to that previously described (Hsu et
541 al., 2016), except that the Araport11 annotation was used in this study. Briefly, for Ribo-seq
542 libraries, the adaptor (AGATCGGAAGAGCACACGTCT) was clipped with fastx_clipper (FASTX
543 toolkit v0.0.14) (http://hannonlab.cshl.edu/fastx_tool- kit/). For both RNA-seq and Ribo-seq, we
544 used Bowtie2 (v2.3.4.1) (Langmead and Salzberg, 2012) to remove
545 rRNA/tRNA/snRNA/snoRNA sequences. Both the RNA-seq and Ribo-seq reads were mapped
546 to the transcriptome with STAR aligner (Dobin et al., 2013) (RNA-seq parameters: --
547 outFilterMismatchNmax 2 --outFilterMultimapNmax 20 --outFilterType BySJout --

548 alignSJoverhangMin 8 --alignSJDBoverhangMin 2; all parameters used for Ribo-seq were the
549 same except --outFilterMismatchNmax 1). We then used the bam files from both RNA-seq and
550 Ribo-seq for RiboTaper (v1.3.1a) (Calviello et al., 2016) to identify translated ORFs. The
551 distribution of Ribo-seq reads in different genome features was calculated using Ribo-seQC.
552 The Ribo-seq metaplot was created using the create_metaplots.bash function in RiboTaper.
553 The Ribo-seq read lengths and offsets for RiboTaper were 24, 25, 26, 27, 28 and 8, 9, 10, 11,
554 12, respectively. Combining both 20-min and 60-min samples, the total reads mapped to the
555 genome for Ribo-seq and RNA-seq were 298.01 million and 180.67 million, respectively. The
556 discovered uORFs and mORFs were extracted from the RiboTaper output ORF_max_filt file. To
557 calculate translation efficiency, we first used STAR to map the RNA-seq and Ribo-seq reads to
558 the CDS of annotated coding genes. The resulting bam files were used to quantify the
559 transcripts per million (TPM) of each gene with RSEM (v1.3.1) (Li and Dewey, 2011). Then,
560 translation efficiency was calculated by dividing the Ribo-seq TPM by the RNA-seq TPM. The
561 root and shoot data from Hsu et al., 2016 (Hsu et al., 2016) were reanalyzed using the
562 Araport11 annotation. The P_sites_all files from RiboTaper were processed using the following
563 code: cut -f 1,3,6 P_sites_all | sort | uniq -c | sed -r 's/^(*[^]+) +/\1\t/' > output.txt to combine the
564 read counts at each P-site. Data visualization and statistical analysis were performed in R
565 (v4.0.3) (R Core Team (2013), 2017). In particular, the gene levels from the Ribo-seq and RNA-
566 seq reads were visualized with RiboPlotR (Wu and Hsu, 2021).
567
568 The mRNA half-life and mRNA decay rate data were downloaded from Szabo et al. and
569 Sorenson et al., respectively (Szabo et al., 2020; Sorenson et al., 2018). The quantitative
570 proteomics data for Arabidopsis shoots and roots were downloaded from Song et al. (Song et
571 al., 2018). The expression levels (TPM) used for investigating mRNA levels of uORF genes in
572 different tissues, developmental stages, and ecotypes in Arabidopsis and in tomato were
573 directly downloaded from the EMBO-EBI expression atlas (E-MTAB-7978: Arabidopsis tissue
574 atlas, E-GEOD-53197: 17 Arabidopsis thaliana accessions, E-MTAB-4812: tomato root, leaf,
575 flower [two stages], and fruit [six stages], and E-MTAB-4813: three longitudinal sections of six
576 stages during tomato fruit development) (Papatheodorou et al., 2020). Our previous Ribo-seq
577 and RNA-seq data for Arabidopsis roots and shoots were described in (Hsu et al., 2016); our
578 previous Ribo-seq and RNA-seq data for tomato roots were described in (Wu et al., 2019). The
579 published RNA-seq data for the NMD mutants *upf1* (*lba1*) *upf3-1* and its wild-type control (GEO:
580 GSE41432), *smg7-1 pad4* and its *pad4* control (GEO: GSE55884), *upf1-3 pad4* and its *pad4*
581 control (GEO: GSE146340), and *upf2-10* and its wild-type control (SRA: SRP056795) were

582 downloaded, and the mRNA levels were quantified by Kalisto (Bray et al., 2016) and the TPM
583 values were further analyzed to compare the steady-state mRNA levels in different categories of
584 genes.
585
586 **AVAILABILITY OF DATA AND MATERIALS**
587 All raw and processed sequencing data generated in this study have been submitted to the
588 NCBI Gene Expression Omnibus (GEO; https://www.ncbi.nlm.nih.gov/geo/) under accession
589 number GSE183264. The genomic locations of TuORFs are available on TAIR genome browser
590 (https://www.arabidopsis.org). Codes for this study are available at
591 https://github.com/hsinyenwu/TuORF_vs_NMD_2022.
592
593 **COMPETING INTEREST STATEMENT**
594 The authors declare that they have no competing interests.
595
596 **AUTHOR CONTRIBUTIONS AND ACKNOWLEDGEMENTS**
597 HLW and PYH designed the research, PYH performed the sequencing experiments, HLW
598 analyzed the sequencing data, HLW and PYH interpreted the data, and HLW and PYH wrote
599 the paper. We thank Robert Last and Melissa Lehti-Shiu for critical reading and helpful
600 comments on the manuscript. This work used the Vincent J. Coates Genomics Sequencing
601 Laboratory at UC Berkeley, supported by an NIH S10 OD018174 Instrumentation Grant. This
602 work was supported by a National Science Foundation grant (2051885) and a Michigan State
603 University startup grant to PYH.
604
605 **REFERENCES**
606 **Andreev, D.E., Arnold, M., Kiniry, S.J., Loughran, G., Michel, A.M., Rachinskii, D., and**
607 **Baranov, P. V.** (2018). TASEP modelling provides a parsimonious explanation for the
608 ability of a single uORF to derepress translation during the integrated stress response.
609 eLife **7**: e32563.
610 **Von Arnim, A.G., Jia, Q., and Vaughn, J.N.** (2014). Regulation of plant translation by
611 upstream open reading frames. Plant Science **214**: 1–12.
612 **Baird, T.D., Cheng, K.C.C., Chen, Y.C., Buehler, E., Martin, S.E., Inglese, J., and Hogg, J.R.**
613 (2018). ICE1 promotes the link between splicing and nonsense-mediated mRNA decay.
614 eLife **7**.
615 **Bazin, J., Baerenfaller, K., Gosai, S.J., Gregory, B.D., Crespi, M., and Bailey-Serres, J.**

616 (2017). Global analysis of ribosome-associated noncoding RNAs unveils new modes of
617 translational regulation. Proceedings of the National Academy of Sciences of the United
618 States of America **114**: E10018–E10027.
619 **Beelman, C.A. and Parker, R.** (1994). Differential effects of translational inhibition in cis and in
620 trans on the decay of the unstable yeast MFA2 mRNA. Journal of Biological Chemistry
621 **269**: 9687–9692.
622 **Boudsocq, M., Barbier-Brygoo, H., and Laurière, C.** (2004). Identification of nine sucrose
623 nonfermenting 1-related protein kinases 2 activated by hyperosmotic and saline stresses in
624 Arabidopsis thaliana. Journal of Biological Chemistry **279**: 41758–41766.
625 **Brar, G.A. and Weissman, J.S.** (2015). Ribosome profiling reveals the what, when, where and
626 how of protein synthesis. Nature Reviews Molecular Cell Biology **16**: 651–664.
627 **Bray, N.L., Pimentel, H., Melsted, P., and Pachter, L.** (2016). Near-optimal probabilistic RNA-
628 seq quantification. Nature biotechnology **34**: 525–527.
629 **Cai, Q., Fukushima, H., Yamamoto, M., Ishii, N., Sakamoto, T., Kurata, T., Motose, H., and**
630 **Takahashi, T.** (2016). The SAC51 family plays a central role in thermospermine responses
631 in arabidopsis. Plant and Cell Physiology **57**: 1583–1592.
632 **Calviello, L., Mukherjee, N., Wyler, E., Zauber, H., Hirsekorn, A., Selbach, M., Landthaler,**
633 **M., Obermayer, B., and Ohler, U.** (2016). Detecting actively translated open reading
634 frames in ribosome profiling data. Nature Methods **13**: 165–170.
635 **Calvo, S.E., Pagliarini, D.J., and Mootha, V.K.** (2009). Upstream open reading frames cause
636 widespread reduction of protein expression and are polymorphic among humans.
637 Proceedings of the National Academy of Sciences of the United States of America **106**:
638 7507–7512.
639 **Chan, L.Y., Mugler, C.F., Heinrich, S., Vallotton, P., and Weis, K.** (2018). Non-invasive
640 measurement of mRNA decay reveals translation initiation as the major determinant of
641 mRNA stability. eLife **7**: e32536.
642 **Chang, H.M., Triboulet, R., Thornton, J.E., and Gregory, R.I.** (2013). A role for the Perlman
643 syndrome exonuclease Dis3l2 in the Lin28-let-7 pathway. Nature **497**: 244–248.
644 **Chew, G.L., Pauli, A., and Schier, A.F.** (2016). Conservation of uORF repressiveness and
645 sequence features in mouse, human and zebrafish. Nature Communications **7**: 11663.
646 **Chiam, N.-C., Fujimura, T., Sano, R., Akiyoshi, N., Hiroyama, R., Watanabe, Y., Motose, H.,**
647 **Demura, T., and Ohtani, M.** (2019). Nonsense-Mediated mRNA Decay Deficiency Affects
648 the Auxin Response and Shoot Regeneration in Arabidopsis. Plant and Cell Physiology **60**:
649 2000–2014.

650 **Clarke, J.T., Warnock, R.C.M., and Donoghue, P.C.J.** (2011). Establishing a time-scale for
651 plant evolution. The New Phytologist **192**: 266–301.
652 **Cui, X., Lv, Y., Chen, M., Nikoloski, Z., Twell, D., and Zhang, D.** (2015). Young genes out of
653 the male: An insight from evolutionary age analysis of the pollen transcriptome. Molecular
654 Plant **8**: 935–945.
655 **Degtiar, E., Fridman, A., Gottlieb, D., Vexler, K., Berezin, I., Farhi, R., Golani, L., and**
656 **Shaul, O.** (2015). The feedback control of UPF3 is crucial for RNA surveillance in plants.
657 Nucleic Acids Research **43**: 4219–4235.
658 **Dever, T.E., Ivanov, I.P., and Sachs, M.S.** (2020). Conserved Upstream Open Reading Frame
659 Nascent Peptides That Control Translation. Annual Review of Genetics **54**: 237–264.
660 **Devlin, P.F., Patel, S.R., and Whitelam, G.C.** (1998). Phytochrome E Influences Internode
661 Elongation and Flowering Time in Arabidopsis. The Plant Cell **10**: 1479–1487.
662 **Deyholos, M.K., Cavaness, G.F., Hall, B., King, E., Punwani, J., Van Norman, J., and**
663 **Sieburth, L.E.** (2003). Varicose, a WD-domain protein, is required for leaf blade.
664 Development **130**: 6577–6588.
665 **Dobin, A., Davis, C.A., Schlesinger, F., Drenkow, J., Zaleski, C., Jha, S., Batut, P.,**
666 **Chaisson, M., and Gingeras, T.R.** (2013). STAR: ultrafast universal RNA-seq aligner.
667 Bioinformatics **29**: 15–21.
668 **Drechsel, G., Kahles, A., Kesarwani, A.K., Stauffer, E., Behr, J., Drewe, P., Rätsch, G., and**
669 **Wachter, A.** (2013). Nonsense-mediated decay of alternative precursor mRNA splicing
670 variants is a major determinant of the Arabidopsis steady state transcriptome. The Plant
671 Cell **25**: 3726–3742.
672 **Ellis, C.M., Nagpal, P., Young, J.C., Hagen, G., Guilfoyle, T.J., and Reed, J.W.** (2005).
673 AUXIN RESPONSE FACTOR1 and AUXIN RESPONSE FACTOR2 regulate senescence
674 and floral organ abscission in Arabidopsis thaliana. Development **132**: 4563–4574.
675 **Filichkin, S.A., Cumbie, J.S., Dharmawardhana, P., Jaiswal, P., Chang, J.H., Palusa, S.G.,**
676 **Reddy, A.S.N., Megraw, M., and Mockler, T.C.** (2015). Environmental stresses modulate
677 abundance and timing of alternatively spliced circadian transcripts in Arabidopsis.
678 Molecular Plant **8**: 207–227.
679 **Gloggnitzer, J., Akimcheva, S., Srinivasan, A., Kusenda, B., Riehs, N., Stampfl, H., Bautor,**
680 **J., Dekrout, B., Jonak, C., Jiménez-Gómez, J.M., Parker, J.E., and Riha, K.** (2014).
681 Nonsense-mediated mRNA decay modulates immune receptor levels to regulate plant
682 antibacterial defense. Cell Host and Microbe **16**: 376–390.
683 **Goeres, D.C., Van Norman, J.M., Zhang, W., Fauver, N.A., Spencer, M. Lou, and Sieburth,**

684 **L.E.** (2007). Components of the Arabidopsis mRNA decapping complex are required for
685 early seedling development. The Plant Cell **19**: 1549–1564.
686 **Harnett, D., Meerdink, E., Calviello, L., Sydow, D., and Ohler, U.** (2021). Genome-Wide
687 Analysis of Actively Translated Open Reading Frames Using RiboTaper/ORFquant.
688 Methods in Molecular Biology **2252**: 331–346.
689 **Hayden, C.A. and Jorgensen, R.A.** (2007). Identification of novel conserved peptide uORF
690 homology groups in Arabidopsis and rice reveals ancient eukaryotic origin of select groups
691 and preferential association with transcription factor-encoding genes. BMC Biology **5**: 32.
692 **He, F. and Jacobson, A.** (2015). Nonsense-Mediated mRNA Decay: Degradation of Defective
693 Transcripts Is only Part of the Story. Annual Review of Genetics **49**: 339–366.
694 **Hinnebusch, A.G., Ivanov, I.P., and Sonenberg, N.** (2016). Translational control by 5′-
695 untranslated regions of eukaryotic mRNAs. Science **352**: 1413–1416.
696 **Van Der Horst, S., Snel, B., Hanson, J., and Smeekens, S.** (2019). Novel pipeline identifies
697 new upstream ORFs and non-AUG initiating main ORFs with conserved amino acid
698 sequences in the 5′ leader of mRNAs in Arabidopsis thaliana. RNA **25**: 292–304.
699 **Hou, C.-Y., Lee, W.-C., Chou, H.-C., Chen, A.-P., Chou, S.-J., and Chen, H.-M.** (2016).
700 Global analysis of truncated RNA ends reveals new insights into ribosome stalling in
701 plants. The Plant Cell **28**: 2398–2416.
702 **Hsu, P.Y., Calviello, L., Wu, H.-Y.L., Li, F.-W., Rothfels, C.J., Ohler, U., and Benfey, P.N.**
703 (2016). Super-resolution ribosome profiling reveals unannotated translation events in
704 Arabidopsis. Proceedings of the National Academy of Sciences of the United States of
705 America **113**: E7126–E7135.
706 **Hu, Q., Merchante, C., Stepanova, A.N., Alonso, J.M., and Heber, S.** (2016). Genome-Wide
707 Search for Translated Upstream Open Reading Frames in Arabidopsis Thaliana. IEEE
708 Transactions on Nanobioscience **15**: 150–159.
709 **Huq, E. and Quail, P.H.** (2002). PIF4, a phytochrome-interacting bHLH factor, functions as a
710 negative regulator of phytochrome B signaling in Arabidopsis. EMBO Journal **21**: 2441–
711 2450.
712 **Hurt, J.A., Robertson, A.D., and Burge, C.B.** (2013). Global analyses of UPF1 binding and
713 function reveal expanded scope of nonsense-mediated mRNA decay. Genome Research
714 **23**: 1636–1650.
715 **Imai, A., Hanzawa, Y., Komura, M., Yamamoto, K.T., Komeda, Y., and Takahashi, T.** (2006).
716 The dwarf phenotype of the Arabidopsis acl5 mutant is suppressed by a mutation in an
717 upstream ORF of a bHLH gene. Development **133**: 3575–3585.

718 **Ingolia, N.T., Ghaemmaghami, S., Newman, J.R.S., and Weissman, J.S.** (2009). Genome-
719 wide analysis in vivo of translation with nucleotide resolution using ribosome profiling.
720 Science **324**: 218–223.
721 **Isken, O., Kim, Y.K., Hosoda, N., Mayeur, G.L., Hershey, J.W.B., and Maquat, L.E.** (2008).
722 Upf1 Phosphorylation Triggers Translational Repression during Nonsense-Mediated mRNA
723 Decay. Cell **133**: 314–327.
724 **Jeong, H.J., Kim, Y.J., Kim, S.H., Kim, Y.H., Lee, I.J., Kim, Y.K., and Shin, J.S.** (2011).
725 Nonsense-mediated mRNA decay factors, UPF1 and UPF3, contribute to plant defense.
726 Plant and Cell Physiology **52**: 2147–2156.
727 **Johnstone, T.G., Bazzini, A.A., and Giraldez, A.J.** (2016). Upstream ORFs are prevalent
728 translational repressors in vertebrates. The EMBO Journal **35**: 706–723.
729 **Jorgensen, R.A. and Dorantes-Acosta, A.E.** (2012). Conserved peptide upstream open
730 reading frames are associated with regulatory genes in angiosperms. Frontiers in Plant
731 Science **3**: 191.
732 **Juntawong, P., Girke, T., Bazin, J., and Bailey-Serres, J.** (2014). Translational dynamics
733 revealed by genome-wide profiling of ribosome footprints in Arabidopsis. Proceedings of
734 the National Academy of Sciences of the United States of America **111**: E203–E212.
735 **Kalyna, M. et al.** (2012). Alternative splicing and nonsense-mediated decay modulate
736 expression of important regulatory genes in Arabidopsis. Nucleic Acids Research **40**:
737 2454–2469.
738 **Kerényi, F., Wawer, I., Sikorski, P.J., Kufel, J., and Silhavy, D.** (2013). Phosphorylation of
739 the N- and C-terminal UPF1 domains plays a critical role in plant nonsense-mediated
740 mRNA decay. Plant Journal **76**: 836–848.
741 **Kertész, S., Kerényi, Z., Mérai, Z., Bartos, I., Pálfy, T., Barta, E., and Silhavy, D.** (2006).
742 Both introns and long 3′-UTRs operate as cis-acting elements to trigger nonsense-
743 mediated decay in plants. Nucleic Acids Research **34**: 6147–6157.
744 **Kim, B.H., Cai, X., Vaughn, J.N., and Von Arnim, A.G.** (2007). On the functions of the h
745 subunit of eukaryotic initiation factor 3 in late stages of translation initiation. Genome
746 Biology **8**: R60.
747 **Kozak, M.** (1999). Initiation of translation in prokaryotes and eukaryotes. Gene **234**: 187–208.
748 **Kurihara, Y. et al.** (2009). Genome-wide suppression of aberrant mRNA-like noncoding RNAs
749 by NMD in Arabidopsis. Proceedings of the National Academy of Sciences of the United
750 States of America **106**: 2453–2458.
751 **Kurihara, Y., Makita, Y., Kawashima, M., Fujita, T., Iwasaki, S., and Matsui, M.** (2018).

752 Transcripts from downstream alternative transcription start sites evade uORF-mediated
753 inhibition of gene expression in Arabidopsis. Proceedings of the National Academy of
754 Sciences of the United States of America **115**: 7831–7836.
755 **Kurihara, Y., Makita, Y., Shimohira, H., Fujita, T., Iwasaki, S., and Matsui, M.** (2020).
756 Translational landscape of protein-coding and non-protein-coding RNAs upon light
757 exposure in Arabidopsis. Plant and Cell Physiology **61**: 536–545.
758 **Kurosaki, T., Li, W., Hoque, M., Popp, M.W.L., Ermolenko, D.N., Tian, B., and Maquat, L.E.**
759 (2014). A Post-Translational regulatory switch on UPF1 controls targeted mRNA
760 degradation. Genes and Development **28**: 1900–1916.
761 **Kurosaki, T., Popp, M.W., and Maquat, L.E.** (2019). Quality and quantity control of gene
762 expression by nonsense-mediated mRNA decay. Nature Reviews Molecular Cell Biology
763 2019 20:7 **20**: 406–420.
764 **LaGrandeur, T. and Parker, R.** (1999). The cis acting sequences responsible for the differential
765 decay of the unstable MFA2 and stable PGK1 transcipts in yeast include the context of the
766 translational start codon. RNA **5**: 420–433.
767 **Langmead, B. and Salzberg, S.L.** (2012). Fast gapped-read alignment with Bowtie 2. Nature
768 Methods **9**: 357–359.
769 **Di Laurenzio, L., Wysocka-Diller, J., Malamy, J.E., Pysh, L., Helariutta, Y., Freshour, G.,**
770 **Hahn, M.G., Feldmann, K.A., and Benfey, P.N.** (1996). The SCARECROW gene
771 regulates an asymmetric cell division that is essential for generating the radial organization
772 of the Arabidopsis root. Cell **86**: 423–433.
773 **Lawson, M.R., Lessen, L.N., Wang, J., Prabhakar, A., Corsepius, N.C., Green, R., and**
774 **Puglisi, J.D.** (2021). Mechanisms that ensure speed and fidelity in eukaryotic translation
775 termination. Science **373**: 876–882.
776 **Lee, D.S.M., Park, J., Kromer, A., Baras, A., Rader, D.J., Ritchie, M.D., Ghanem, L.R., and**
777 **Barash, Y.** (2021). Disrupting upstream translation in mRNAs is associated with human
778 disease. Nature Communications 2021 12:1 **12**: 1–14.
779 **Leivar, P., Monte, E., Al-Sady, B., Carle, C., Storer, A., Alonso, J.M., Ecker, J.R., and Quail,**
780 **P.H.** (2008). The Arabidopsis phytochrome-interacting factor PIF7, together with PIF3 and
781 PIF4, regulates responses to prolonged red light by modulating phyB levels. The Plant Cell
782 **20**: 337–352.
783 **Li, B. and Dewey, C.N.** (2011). RSEM: accurate transcript quantification from RNA-Seq data
784 with or without a reference genome. BMC Bioinformatics **12**: 323.
785 **Li, Y.R. and Liu, M.J.** (2020). Prevalence of alternative AUG and non-AUG translation initiators

786 and their regulatory effects across plants. Genome Research **30**: 1418–1433.
787 **Lin, Y., May, G.E., Kready, H., Nazzaro, L., Mao, M., Spealman, P., Creeger, Y., and Joel**
788 **McManus, C.** (2019). Impacts of uORF codon identity and position on translation
789 regulation. Nucleic Acids Research **47**: 9358–9367.
790 **Liu, M.J., Wu, S.H., Wu, J.F., Lin, W.D., Wu, Y.C., Tsai, T.Y., Tsai, H.L., and Wu, S.H.** (2013).
791 Translational landscape of photomorphogenic Arabidopsis. Plant Cell **25**: 3699–3710.
792 **Lloyd, J.P.B. and Davies, B.** (2013). SMG1 is an ancient nonsense-mediated mRNA decay
793 effector. The Plant journal : for cell and molecular biology **76**: 800–810.
794 **Lubas, M., Damgaard, C.K., Tomecki, R., Cysewski, D., Jensen, T.H., and Dziembowski, A.**
795 (2013). Exonuclease hDIS3L2 specifies an exosome-independent 3'-5' degradation
796 pathway of human cytoplasmic mRNA. The EMBO journal **32**: 1855–1868.
797 **Merchante, C., Brumos, J., Yun, J., Hu, Q., Spencer, K.R., Enríquez, P., Binder, B.M.,**
798 **Heber, S., Stepanova, A.N., and Alonso, J.M.** (2015). Gene-specific translation
799 regulation mediated by the hormone-signaling molecule EIN2. Cell **163**: 684–697.
800 **Mizoguchi, T., Hayashida, N., Yamaguchi-Shinozaki, K., Kamada, H., and Shinozaki, K.**
801 (1995). Two genes that encode ribosomal-protein S6 kinase homologs are induced by cold
802 or salinity stress in Arabidopsis thaliana. FEBS Letters **358**: 199–204.
803 **Nagarajan, V.K., Kukulich, P.M., Von Hagel, B., and Green, P.J.** (2019). RNA degradomes
804 reveal substrates and importance for dark and nitrogen stress responses of Arabidopsis
805 XRN4. Nucleic Acids Research **47**: 9216–9230.
806 **Nagpal, P., Ellis, C.M., Weber, H., Ploense, S.E., Barkawi, L.S., Guilfoyle, T.J., Hagen, G.,**
807 **Alonso, J.M., Cohen, J.D., Farmer, E.E., Ecker, J.R., and Reed, J.W.** (2005). Auxin
808 response factors ARF6 and ARF8 promote jasmonic acid production and flower
809 maturation. Development **132**: 4107–4118.
810 **Ni, M., Tepperman, J.M., and Quail, P.H.** (1998). PIF3, a phytochrome-interacting factor
811 necessary for normal photoinduced signal transduction, is a novel basic helix-loop-helix
812 protein. Cell **95**: 657–667.
813 **Nyikó, T., Sonkoly, B., Mérai, Z., Benkovics, A.H., and Silhavy, D.** (2009). Plant upstream
814 ORFs can trigger nonsense-mediated mRNA decay in a size-dependent manner. Plant
815 Molecular Biology **71**: 367–378.
816 **Ohtani, M. and Wachter, A.** (2019). NMD-Based Gene Regulation - A Strategy for Fitness
817 Enhancement in Plants? Plant and Cell Physiology **60**: 1953–1960.
818 **Papatheodorou, I. et al.** (2020). Expression Atlas update: From tissues to single cells. Nucleic
819 Acids Research **48**: D77–D83.

820 **Park, Y.S., Hong, S.W., Oh, S.A., Kwak, J.M., Lee, H.H., and Nam, H.G.** (1993). Two putative
821 protein kinases from Arabidopsis thaliana contain highly acidic domains. Plant Molecular
822 Biology **22**: 615–624.
823 **Presnyak, V., Alhusaini, N., Chen, Y.H., Martin, S., Morris, N., Kline, N., Olson, S.,**
824 **Weinberg, D., Baker, K.E., Graveley, B.R., and Coller, J.** (2015). Codon optimality is a
825 major determinant of mRNA stability. Cell **160**: 1111–1124.
826 **R Core Team (2013)** (2017). R: A language and environment for statistical computing. R
827 Foundation for Statistical Computing, Vienna, Austria.
828 **Radhakrishnan, A., Chen, Y.H., Martin, S., Alhusaini, N., Green, R., and Coller, J.** (2016).
829 The DEAD-Box Protein Dhh1p Couples mRNA Decay and Translation by Monitoring
830 Codon Optimality. Cell **167**: 122-132.e9.
831 **Raxwal, V.K. and Riha, K.** (2016). Nonsense mediated RNA decay and evolutionary
832 capacitance. Biochimica et Biophysica Acta **1859**: 1538–1543.
833 **Raxwal, V.K., Simpson, C.G., Gloggnitzer, J., Entinze, J.C., Guo, W., Zhang, R., Brown,**
834 **J.W.S., and Riha, K.** (2020). Nonsense-Mediated RNA Decay Factor UPF1 Is Critical for
835 Posttranscriptional and Translational Gene Regulation in Arabidopsis. The Plant Cell **32**:
836 2725–2741.
837 **Rayson, S., Arciga-Reyes, L., Wootton, L., de Torres Zabala, M., Truman, W., Graham, N.,**
838 **Grant, M., and Davies, B.** (2012). A role for nonsense-mediated mrna decay in plants:
839 Pathogen responses are induced in arabidopsis thaliana nmd mutants. PLoS ONE **7**:
840 e31917.
841 **Riehs-Kearnan, N., Gloggnitzer, J., Dekrout, B., Jonak, C., and Riha, K.** (2012). Aberrant
842 growth and lethality of Arabidopsis deficient in nonsense-mediated RNA decay factors is
843 caused by autoimmune-like response. Nucleic Acids Research **40**: 5615–5624.
844 **Saul, H. et al.** (2009). The upstream open reading frame of the Arabidopsis AtMHX gene has a
845 strong impact on transcript accumulation through the nonsense-mediated mRNA decay
846 pathway. The Plant Journal **60**: 1031–1042.
847 **Schwartz, D.C. and Parker, R.** (2000). mRNA Decapping in Yeast Requires Dissociation of the
848 Cap Binding Protein, Eukaryotic Translation Initiation Factor 4E. Molecular and Cellular
849 Biology **20**: 7933–7942.
850 **Shah, P., Ding, Y., Niemczyk, M., Kudla, G., and Plotkin, J.B.** (2013). Rate-Limiting Steps in
851 Yeast Protein Translation. Cell **153**: 1589–1601.
852 **Sharrock, R.A. and Quail, P.H.** (1989). Novel phytochrome sequences in Arabidopsis thaliana:
853 structure, evolution, and differential expression of a plant regulatory photoreceptor family.

854 Genes & Development **3**: 1745–1757.
855 **Sieburth, L.E. and Vincent, J.N.** (2018). Beyond transcription factors: Roles of mrna decay in
856 regulating gene expression in plants [version 1; referees: 3 approved]. F1000Research **7**:
857 1940.
858 **Silverstone, A.L., Ciampaglio, C.N., and Sun, T.P.** (1998). The Arabidopsis RGA gene
859 encodes a transcriptional regulator repressing the gibberellin signal transduction pathway.
860 The Plant Cell **10**: 155–169.
861 **Song, G., Hsu, P.Y., and Walley, J.W.** (2018). Assessment and Refinement of Sample
862 Preparation Methods for Deep and Quantitative Plant Proteome Profiling. Proteomics **18**:
863 e1800220.
864 **Sorenson, R.S., Deshotel, M.J., Johnson, K., Adler, F.R., and Sieburth, L.E.** (2018).
865 Arabidopsis mRNA decay landscape arises from specialized RNA decay substrates,
866 decapping-mediated feedback, and redundancy. Proceedings of the National Academy of
867 Sciences of the United States of America **115**: E1485–E1494.
868 **Strayer, C., Oyama, T., Schultz, T.F., Raman, R., Somers, D.E., Mas, P., Panda, S., Kreps,**
869 **J.A., and Kay, S.A.** (2000). Cloning of the Arabidopsis clock gene TOC1, an
870 autoregulatory response regulator homolog. Science **289**: 768–771.
871 **Szabo, E.X., Reichert, P., Lehniger, M.K., Ohmer, M., de Francisco Amorim, M., Gowik, U.,**
872 **Schmitz-Linneweber, C., and Laubinger, S.** (2020). Metabolic labeling of RNAs uncovers
873 hidden features and dynamics of the Arabidopsis transcriptome. The Plant Cell **32**: 871–
874 887.
875 **Takahashi, H., Takahashi, A., Naito, S., and Onouchi, H.** (2012). BAIUCAS: A novel BLAST-
876 based algorithm for the identification of upstream open reading frames with conserved
877 amino acid sequences and its application to the Arabidopsis thaliana genome.
878 Bioinformatics **28**: 2231–2241.
879 **Tanaka, M., Sotta, N., Yamazumi, Y., Yamashita, Y., Miwa, K., Murota, K., Chiba, Y., Hirai,**
880 **M.Y., Akiyama, T., Onouchi, H., Naito, S., and Fujiwara, T.** (2016). The minimum open
881 reading frame, AUG-Stop, induces boron-dependent ribosome stalling and mRNA
882 degradation. The Plant Cell **28**: 2830–2849.
883 **Uchiyama-Kadokura, N., Murakami, K., Takemoto, M., Koyanagi, N., Murota, K., Naito, S.,**
884 **and Onouchi, H.** (2014). Polyamine-responsive ribosomal arrest at the stop codon of an
885 upstream open reading frame of the AdoMetDC1 gene triggers nonsense-mediated mRNA
886 decay in Arabidopsis thaliana. Plant and Cell Physiology **55**: 1556–1567.
887 **Vaughn, J.N., Ellingson, S.R., Mignone, F., and Arnim, A. von** (2012). Known and novel

888 post-transcriptional regulatory sequences are conserved across plant families. RNA **18**:
889 368–84.
890 **Wolfa, Y.I., Novichkovb, P.S., Kareva, G.P., Koonina, E. V., and Lipmana, D.J.** (2009). The
891 universal distribution of evolutionary rates of genes and distinct characteristics of
892 eukaryotic genes of different apparent ages. Proceedings of the National Academy of
893 Sciences of the United States of America **106**: 7273–7280.
894 **Wu, H.-Y.L. and Hsu, P.Y.** (2021). RiboPlotR: a visualization tool for periodic Ribo-seq reads.
895 Plant Methods **17**: 1–7.
896 **Wu, H.Y.L., Song, G., Walley, J.W., and Hsu, P.Y.** (2019). The tomato translational landscape
897 revealed by transcriptome assembly and ribosome profiling. Plant Physiology **181**: 367–
898 380.
899 **Xu, G., Yuan, M., Ai, C., Liu, L., Zhuang, E., Karapetyan, S., Wang, S., and Dong, X.** (2017).
900 uORF-mediated translation allows engineered plant disease resistance without fitness
901 costs. Nature **545**: 491–494.
902 **Xu, J., Yang, J.Y., Niu, Q.W., and Chua, N.H.** (2006). Arabidopsis DCP2, DCP1, and
903 VARICOSE form a decapping complex required for postembryonic development. The Plant
904 Cell **18**: 3386–3398.
905 **Xu, Z., Hu, L., Shi, B., Geng, S., Xu, L., Wang, D., and Lu, Z.J.** (2018). Ribosome elongating
906 footprints denoised by wavelet transform comprehensively characterize dynamic cellular
907 translation events. Nucleic Acids Research **46**: e109.
908 **Yoine, M., Ohto, M.A., Onai, K., Mita, S., and Nakamura, K.** (2006). The lba1 mutation of
909 UPF1 RNA helicase involved in nonsense-mediated mRNA decay causes pleiotropic
910 phenotypic changes and altered sugar signalling in Arabidopsis. The Plant Journal **47**: 49–
911 62.
912 **Yu, X., Willmann, M.R., Anderson, S.J., and Gregory, B.D.** (2016). Genome-wide mapping of
913 uncapped and cleaved transcripts reveals a role for the nuclear mrna cap-binding complex
914 in cotranslational rna decay in Arabidopsis. The Plant Cell **28**: 2385–2397.
915 **Zhang, H., Si, X., Ji, X., Fan, R., Liu, J., Chen, K., Wang, D., and Gao, C.** (2018). Genome
916 editing of upstream open reading frames enables translational control in plants. Nature
917 Biotechnology **36**: 894–898.
918 **Zhang, H., Wang, Y., Wu, X., Tang, X., Wu, C., and Lu, J.** (2021). Determinants of genome-
919 wide distribution and evolution of uORFs in eukaryotes. Nature Communications **12**: 1–17.
920 **Zhang, S.H., Lawton, M.A., Hunter, T., and Lamb, C.J.** (1994). atpk1, a novel ribosomal
921 protein kinase gene from Arabidopsis. I. Isolation, characterization, and expression.

922 Journal of Biological Chemistry **269**: 17586–17592.
923 **Zhang, W., Murphy, C., and Sieburth, L.E.** (2010). Conserved RNaseII domain protein
924 functions in cytoplasmic mRNA decay and suppresses Arabidopsis decapping mutant
925 phenotypes. Proceedings of the National Academy of Sciences of the United States of
926 America **107**: 15981–15985.
927 **Zinshteyn, B., Sinha, N.K., Enam, S.U., Koleske, B., and Green, R.** (2021). Translational
928 repression of NMD targets by GIGYF2 and EIF4E2. PLoS Genetics **17**: e1009813.
929

930 **FIGURES and FIGURE LEGENDS**

Figure 1

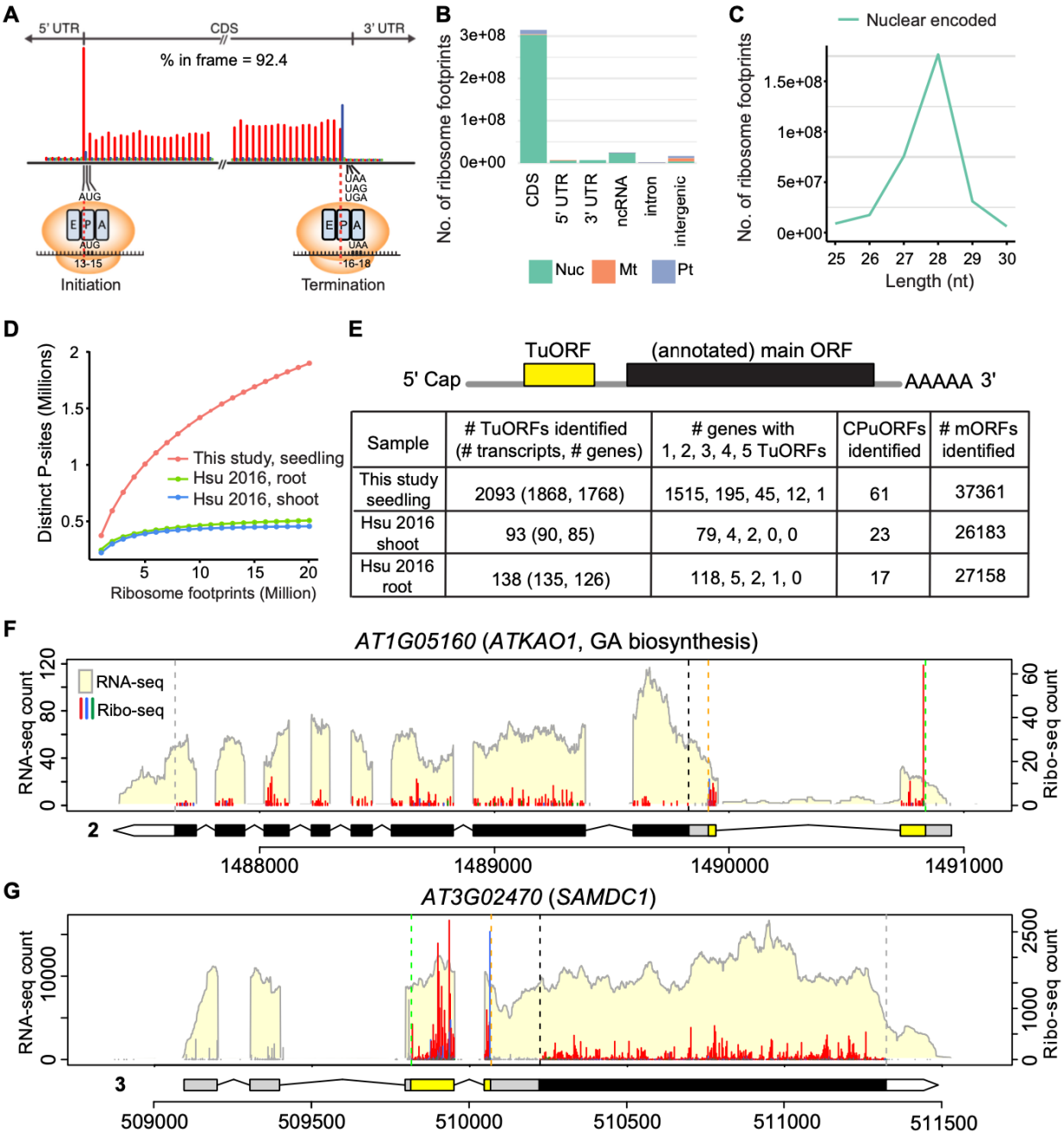

Sample	# TuORFs identified (# transcripts, # genes)	# genes with 1, 2, 3, 4, 5 TuORFs	CPuORFs identified	# mORFs identified
This study seedling	2093 (1868, 1768)	1515, 195, 45, 12, 1	61	37361
Hsu 2016 shoot	93 (90, 85)	79, 4, 2, 0, 0	23	26183
Hsu 2016 root	138 (135, 126)	118, 5, 2, 1, 0	17	27158

931

932 **Figure 1. Enhanced Ribo-seq coverage improves uORF identification**

933 (A) Metagene analysis of 28-nt ribosome footprints mapped to regions near the start and
934 stop codons of annotated ORFs. The reads are presented with their first nt at the P-site,
935 which is the 13th nt for 28-nt footprints. The reads are colored in red, blue, and green to
936 indicate they are in the first (expected), second, and third reading frames, respectively.

937 The majority of footprints were mapped to the CDS in the expected reading frame
938 (92.4% in frame).
939 (B) Genomic features mapped by ribosome footprints. Reads that mapped to nuclear (Nuc)-,
940 mitochondrial (Mt)-, and plastid (Pt)-encoded genes are shown.
941 (C) Length distribution of ribosome footprints. Reads that mapped to nuclear-encoded genes
942 are presented.
943 (D) Distinct P-sites detected in 1 to 20 million randomly selected ribosome footprints from
944 our current and previous datasets.
945 (E) Numbers of TuORFs, CPuORFs, and mORFs identified in our current and previous
946 datasets.
947 (F-G) RNA-seq and Ribo-seq profiles of *ATKAO1 and SAMDC1* from our current data. RNA-
948 seq coverage is shown with a light-yellow background. Ribo-seq reads are presented
949 with their first nt at the P-site, and they are colored in red, blue, and green to indicate
950 they are in the first (expected), second, and third reading frames, respectively. Within the
951 gene models, yellow boxes represent the TuORFs, black boxes represent the annotated
952 mORFs, and gray and white regions indicate 5' UTRs and 3' UTRs, respectively. The
953 specific isoform being considered is indicated to the left of the gene model. Within the
954 profiles, green and orange vertical dashed lines represent translation start and stop,
955 respectively, for the TuORF. Black and gray vertical dashed lines represent translation
956 start and stop, respectively, for the annotated mORF.
957
958
959
960
961
962

Figure 2

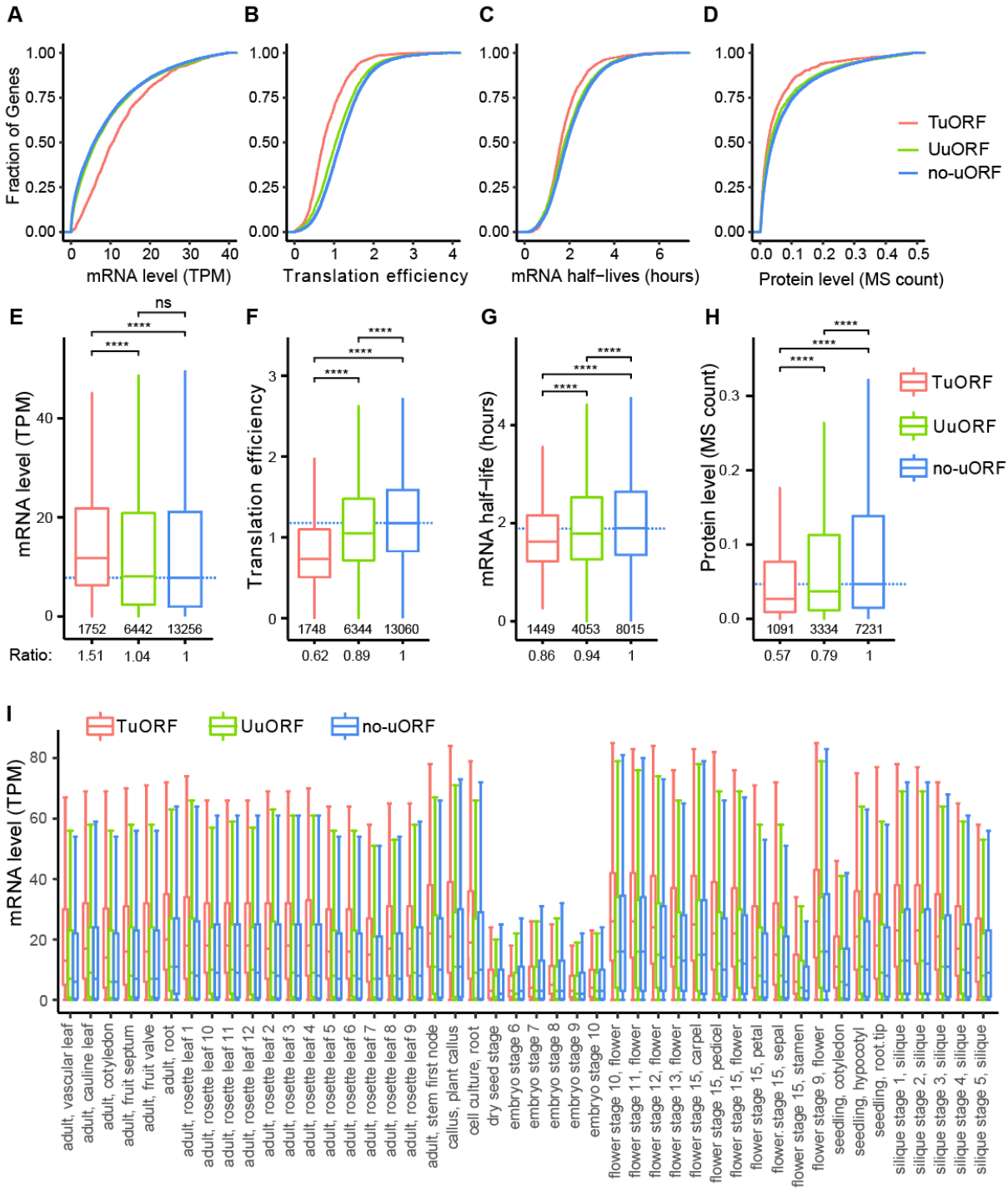

Figure 2. TuORF-containing genes have higher mRNA abundance but are associated with lower translation efficiency, shorter mRNA half-lives, and lower protein abundance

967 (A-D) Cumulative plots and (E-H) boxplots for the mRNA levels, translation efficiency, mRNA
968 half-lives, and protein levels of TuORF, UuORF, and no-uORF genes in Arabidopsis seedlings.
969 The mRNA half-life data, which were measured with metabolic labeling in Arabidopsis
970 seedlings, were extracted from (Szabo et al., 2020), and the protein abundance as determined
971 by quantitative proteomics in Arabidopsis seedling shoots were extracted from (Song et al.,
972 2018). Within the boxplots (E-H), the dashed lines mark the median level of the no-uORF
973 genes; the number of genes in each category is listed below the lower whisker. The ratios
974 underneath the plots indicate the median of each group normalized to that of the no-uORF
975 genes. The statistical significance was determined by Wilcoxon signed-rank test. The adjusted
976 p-value was determined using the Benjamini and Yekutieli procedure to control for the false
977 discovery rate in multiple testing (* 0.05 > p > 0.01, ** 0.01 > p > 0.001, *** 0.001 > p > 1e-4,
978 **** 1e-4 > p > 0). These statistical analyses and graphic layouts were applied to all boxplots in
979 the study.
980 (I) The mRNA levels of TuORF, UuORF, and no-uORF genes in 46 Arabidopsis tissues and
981 developmental stages from independent studies. The TPM values from RNA-seq quantification
982 were downloaded from the EMBO-EBI expression atlas (Papatheodorou et al., 2020). Additional
983 82 Arabidopsis and tomato RNA-seq datasets were presented in Figure S5.
984
985
986

Figure 3

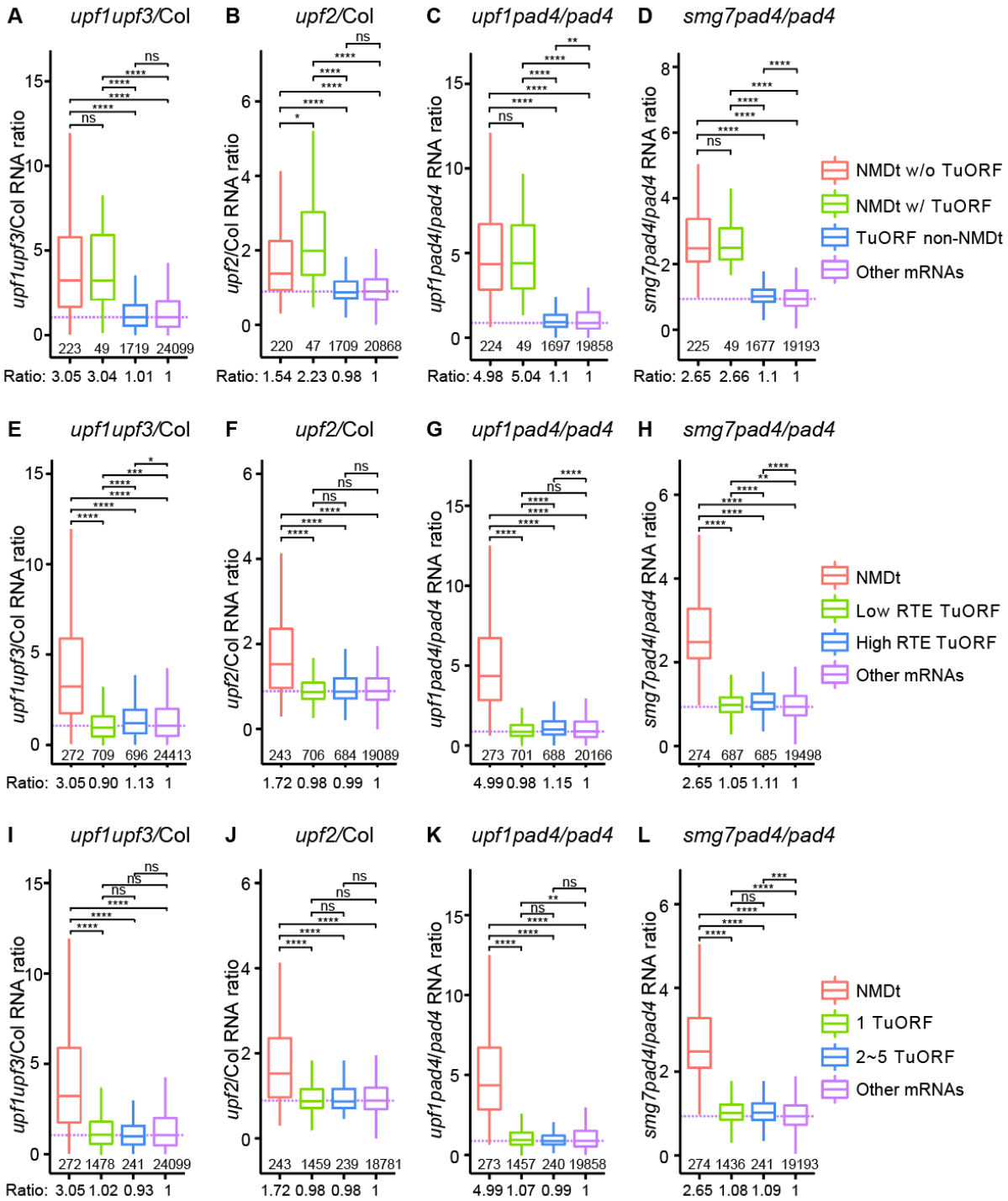

Figure 3: TuORF mRNAs are not upregulated in the NMD mutants

The ratios of mRNA levels between NMD mutants and their control plants from four RNA-seq datasets (Drechsel et al., 2013; Merchante et al., 2015; Raxwal et al., 2020; Gloggnitzer et al., 2014) were used to examine the effects of the NMD pathway on four gene groups: NMD targets

992 without TuORF (NMDt w/o TuORF), NMD targets with TuORF (NMDt w/ TuORF), TuORF
993 mRNAs not identified as NMD targets (TuORF non-NMDt) and other mRNAs. (A) *upf1* (*lba1*
994 allele) *upf3-1* double mutant compared with wild type (Col-0). (B) *upf2-10* compared with wild
995 type (Col-0). (C) *upf1-3 pad4* compared with *pad4*. (D) *smg7-1 pad4* compared with *pad4*. See
996 Table S3 for specific growth conditions for each dataset. (E-H) Same datasets as 4A-D, but the
997 TuORF mRNAs were grouped based on low or high relative TuORF translation efficiency (RTE)
998 (i.e., TE_{TuORF} / TE_{mORF}). (I-L) Same datasets as 4A-D, but the TuORF mRNAs were grouped
999 based on the number of TuORF(s). Within the boxplots, the dashed lines mark the median level
1000 of other mRNAs; the number of genes in each category is listed below the lower whisker. The
1001 ratios underneath the plots indicate the median of each group normalized to that of other
1002 mRNAs. The statistical significance was determined as described in the Figure 2 legend.

Figure 4

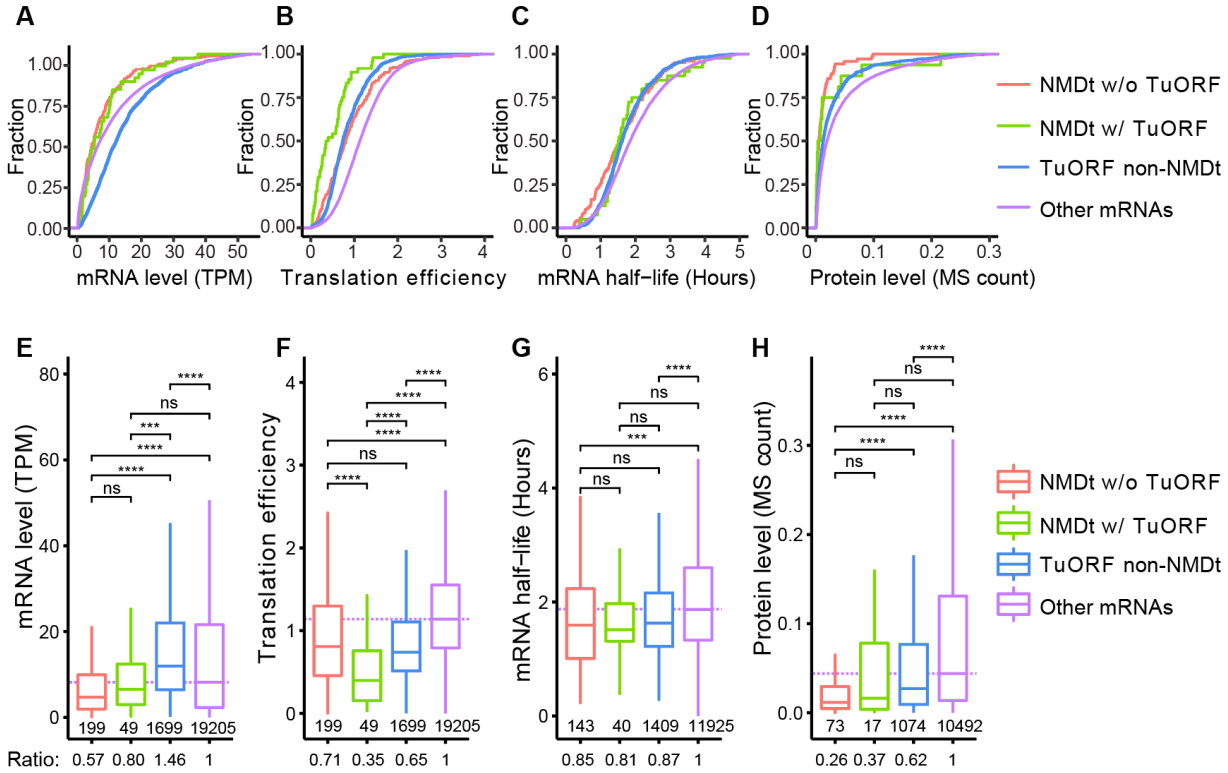

Figure 4. Expression patterns of NMD targets and TuORF mRNAs.
Cumulative plots (A-D) and boxplots (E-H) for the mRNA levels (A, E), translation efficiency (B, F), mRNA half-lives (C, G), and protein levels (D, H) of NMD targets (NMDt) without or with TuORFs compared with those of TuORF mRNAs not identified as NMD targets and other mRNAs. Within the boxplots, the dashed lines mark the median level of other mRNAs; the number of genes in each category is listed below the lower whisker. The ratios underneath the plots indicate the median of each group normalized to that of other mRNAs. The statistical significance was determined as described in the Figure 2 legend.

Figure 5

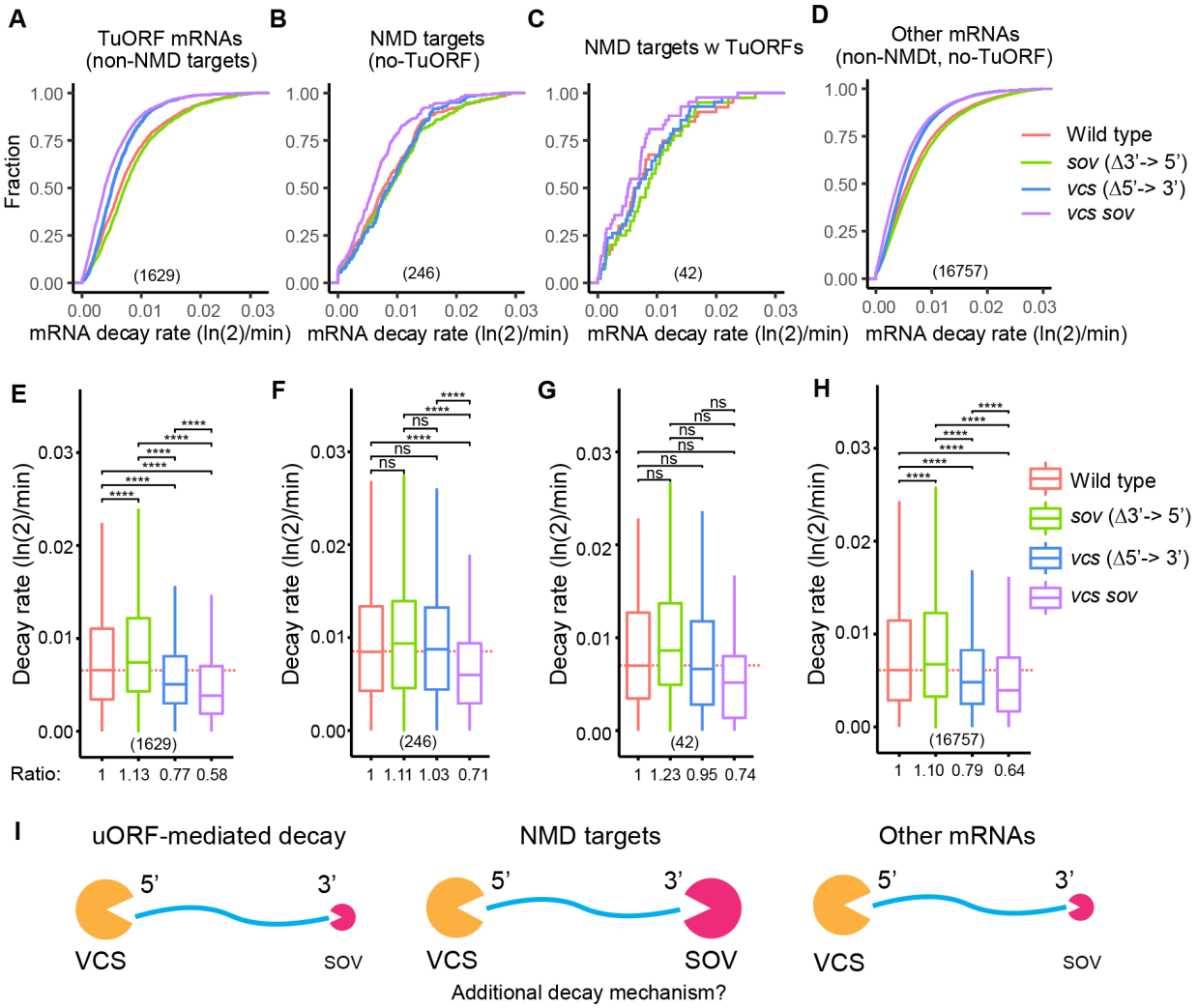

Figure 5. TuORF mRNAs and NMD targets are degraded through different mRNA decay mechanisms

Cumulative plots (A-D) and boxplots (E-H) showing the mRNA decay rates for NMD targets and TuORF mRNAs in wild type and mutants defective in either 5' to 3' decay (*vcs-7*), 3' to 5' decay (*sov*), or both (*vcs sov).* The mRNA decay rates were extracted from (Sorenson et al., 2018). Because Col-0 is naturally an *sov* mutant, the wild type here is Col-0 carrying the functional *SOV* allele from Landsberg *erecta* driven by its native promoter (Zhang et al., 2010; Goeres et al., 2007). The *sov* mutant here is Col-0, and *vcs* is Col-0 with the *vsc-7* allele and the L*er SOV* transgene. The *vcs sov* double mutant is Col-0 carrying the *vcs-7* mutation (Sorenson et al., 2018). Within the boxplots, the dashed lines mark the median level of wild type; the number of genes in each category is listed below the lower whisker. The ratios underneath the plots indicate the median of each group normalized to that of wild type. The statistical significance

1027 was determined as described in the Figure 2 legend. (I) Model of mRNA decay for NMD targets,
1028 TuORF mRNAs, and other mRNAs. The orange packman indicates 5'-to-3' decay machinery,
1029 and the hot pink packman indicates 3'-to-5' decay machinery.
1030

1031 **SUPPLEMENTARY DATA**

1032 **Figure S1.** Correlations among samples and comparisons between our previous and current
1033 datasets

1034 **Figure S2.** Examples of TuORFs in important regulatory genes.

1035 **Figure S3.** Protein abundance of the uORF-containing genes in Arabidopsis root

1036 **Figure S4.** The mRNA levels and translation efficiency of TuORF mRNAs in tomato

1037 **Figure S5.** mRNA levels of uORF-containing genes in different ecotypes, growth stages, and
1038 tissues in Arabidopsis and tomato

1039 **Figure S6.** mRNA levels of CPuORF-containing genes compared to those of no-uORF genes

1040 **Figure S7.** TuORF genes are larger than other genes

1041 **Figure S8.** Lengths of the uORF peptides for NMD target and non-NMD target TuORFs

1042 **Figure S9.** Lengths of UTRs and CDS for NMD targets and TuORF genes

1043 **Figure S10.** The mRNA decay rates of NMD targets and TuORF-containing mRNAs in different
1044 genetic backgrounds

1045 **Table S1**. Translated ORFs identified by RiboTaper

1046 - **Table S1A-C.** Translated uORFs identified in the current dataset and our previous
1047 Arabidopsis shoot and root datasets
1048 - **Table S1D-F.** Translated mORFs identified in the current dataset and our previous
1049 Arabidopsis shoot and root datasets

1050 **Table S2.** GO-term analysis of TuORF genes

1051 **Table S3.** Summary of the large-scale datasets used in this study

1052 **Table S4.** NMD target gene list

1053 - **Table S4A.** High-confidence NMD targets expressed in our data
1054 - **Table S4B.** 49 genes identified as high-confidence NMD target TuORF genes

1055